

PDE-CNNs: Axiomatic Derivations and Applications

Gijs Bellaard, Sei Sakata, Bart M. N. Smets, Remco Duits

Department of Mathematics and Computer Science, CASA, Eindhoven University of Technology, Eindhoven, The Netherlands.

*Corresponding author(s). E-mail(s): g.bellaard@tue.nl;

Contributing authors: s.sakata@student.tue.nl; b.m.n.smets@tue.nl; r.duits@tue.nl;

Abstract

PDE-based Group Convolutional Neural Networks (PDE-G-CNNs) utilize solvers of geometrically meaningful evolution PDEs as substitutes for the conventional components in G-CNNs. PDE-G-CNNs offer several key benefits all at once: fewer parameters, inherent equivariance, better performance, data efficiency, and geometric interpretability.

In this article we focus on Euclidean equivariant PDE-G-CNNs where the feature maps are two dimensional throughout. We call this variant of the framework a PDE-CNN.

From a machine learning perspective, we list several practically desirable axioms and derive from these which PDEs should be used in a PDE-CNN. Here our approach to geometric learning via PDEs is inspired by the axioms of classical linear and morphological scale-space theory, which we generalize by introducing semifield-valued signals.

Furthermore, we experimentally confirm for small networks that PDE-CNNs offer fewer parameters, increased performance, and better data efficiency when compared to CNNs. We also investigate what effect the use of different semifields has on the performance of the models.

Keywords: PDE, Scale-Space, Semifields, Equivariance, Neural Networks, Machine Learning, Computer Vision, Convolution, Tropical Semiring, Morphology

1 Introduction

1.1 Background

Recently, PDE-based group equivariant convolution neural networks (PDE-G-CNNs) [1] were introduced. PDE-G-CNNs belong to the broad family of group equivariant convolution neural networks (G-CNNs) [2]. Unlike traditional CNNs, PDE based networks replace the usual components that make up a CNN layer, that being convolutions, max pooling, and non-linear activation functions, by solvers of evolution PDEs. The coefficients that govern the effect of the PDEs

serve as the trainable parameters. Figure 1 contains a diagram of an example CNN layer and PDE layer, intended to illustrate the similarities and differences between them. Figure 2 visualizes some of the feature maps from trained networks that utilize either standard CNN layers or PDE layers.

It is shown in [1, 4–6] that PDE-G-CNNs – in addition to being inherently equivariant – require fewer parameters, have increased performance, are more data efficient, and more geometrically interpretable, when compared to G-CNNs and classical CNNs. Regarding the geometric interpretability, there is a relation between PDE-G-CNNs and

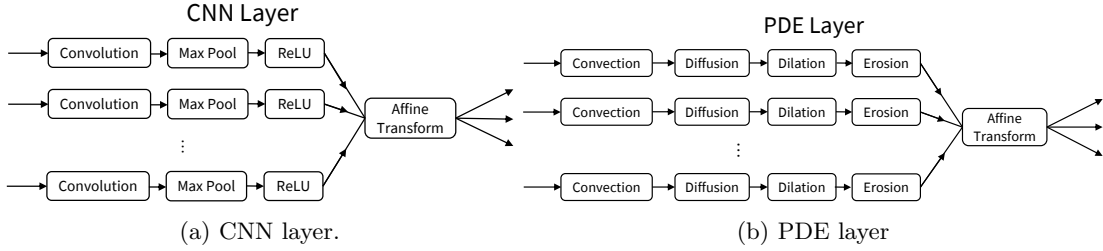


Fig. 1: Diagram of an example CNN layer and PDE layer.

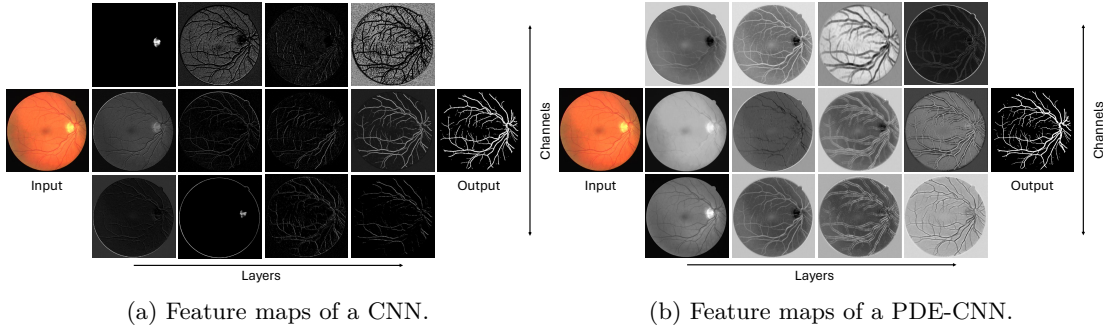


Fig. 2: Illustration of (some of) the feature maps of a standard CNN and a PDE-CNN (both with 6 layers and 16 channels) trained to perform vessel segmentation of images of the fundus of the eye [3]. Not all channels and layers are visualized; a representative selection was chosen. Notice how the feature maps of the PDE-CNN are generally less noisy and more interpretable than those of the CNN. For example, the third picture of the third row of Figure 2b is clearly an edge detector.

association fields [7] from neurogeometry [8, 9], further clarified in [5].

The PDE-G-CNN architecture is very general in the sense that the signals can be defined on *any* Lie group G . However, the existing PDE-G-CNN literature [1, 4–6] mainly concerns itself with $G = \text{SE}(2)$, the group of two-dimensional rotations and translations. We will *not* consider the general setting, or $G = \text{SE}(2)$ for that matter, and restrict ourselves to $G = \mathbb{R}^2$, i.e. standard two-dimensional Euclidean space, for simplicity. We call this specific instance a PDE-CNN. Working with PDE-CNNs, in comparison to the $G = \text{SE}(2)$ based networks, has the advantage of consuming less memory, and the disadvantage that only translation equivariance is included and not rotation equivariance.

In [1] the PDEs that are used in the PDE-G-CNN architecture are convection, diffusion, dilation, and erosion. These PDEs respectively correspond to shifting, blurring, max pooling,

and min pooling. The first question that immediately arises is: **why were these particular PDEs selected?** The quick answer is that these PDEs (except for the convection) come directly from the world of *scale-space theory*. This is what makes PDE-G-CNNs more geometrically meaningful than traditional convolution networks, resulting in more interpretable and less noisy feature maps as can be seen in Figure 2. To appreciate this answer we need to provide the appropriate background by introducing the concept of scale-space representations.

Real world scenes contain many different objects at different scales. When a computer is tasked with analyzing an image of a scene there is no way for it to know beforehand at which scale(s) the interesting structures live. One way to tackle this problem is to analyze the image of interest at *all* scales.

In broad terms, a *scale-space representation* of an image is an ordered collection of images

where each successive image contains less and less detail; that is the smaller scales have been processed away. The collection of images is usually indexed by the *scale-parameter* $t \geq 0$ with $t = 0$ being the original image. In the abstract ideal the scale parameter t is continuous and the scale-space ranges all the way from scale $t = 0$ to scales that are arbitrarily large. In practice a discrete set of scales t is chosen, usually in an exponential manner such as $t = 1, 4, 16, 64, 256$ [10].

The prototypical, and most likely first [11–13], example of a scale-space is the *Gaussian scale-space* made by successive *diffusing* (i.e. *blurring* or *smoothing*) of the original image. The Gaussian scale-space f_t of a two-dimensional image $f_0 : \mathbb{R}^2 \rightarrow \mathbb{R}$ can be written as a *linear convolution* $*$ with a Gaussian *kernel* k_t :

$$\begin{aligned} f_t &= k_t * f_0, \quad k_t(x) = \frac{1}{2\pi t} \exp\left(-\frac{\|x\|^2}{2t}\right), \\ (k_t * f_0)(x) &= \int_{\mathbb{R}^2} k_t(x-y) f_0(y) dy. \end{aligned} \quad (1)$$

Two other examples are the *quadratic morphological scale-space* representations [14] made by successively *dilating* or *eroding* the original image. The quadratic dilation scale-space can be written as a non-linear *dilating convolution* \boxplus with a quadratic kernel:

$$\begin{aligned} f_t &= k_t \boxplus f_0, \quad k_t(x) = -\frac{\|x\|^2}{2t}, \\ (k_t \boxplus f_0)(x) &= \sup_{y \in \mathbb{R}^2} k_t(x-y) + f_0(y). \end{aligned} \quad (2)$$

The quadratic erosion scale-space is created using an *eroding convolution* \boxminus :

$$\begin{aligned} f_t &= k_t \boxminus f_0, \quad k_t(x) = \frac{\|x\|^2}{2t}, \\ (k_t \boxminus f_0)(x) &= \inf_{y \in \mathbb{R}^2} k_t(x-y) + f_0(y). \end{aligned} \quad (3)$$

The dilating and eroding convolutions are collected under the umbrella term *morphological convolution*. This is because they are related by the identity $-(-f \boxplus -g) = f \boxminus g$. The dilating and eroding convolutions can be seen as continuous versions of the max and min-pooling that is commonly used in CNNs.

In Figure 3 the Gaussian, quadratic dilation, and quadratic erosion scale-spaces representations

are visualized of a grayscale image of the fundus of the eye [3].

The Gaussian, quadratic dilation, and quadratic erosion scale-space representations can also be concisely described as the solution to an evolution PDE, with the input image being the initial condition. Namely, the Gaussian scale-space corresponds to the diffusion PDE $\frac{\partial f}{\partial t} = \frac{1}{2}\Delta f$, where Δ is the Laplacian, the quadratic dilation scale-space is the (viscosity¹) solution of dilation PDE $\frac{\partial f}{\partial t} = \frac{1}{2}\|\nabla f\|^2$, and the quadratic erosion corresponds to the erosion PDE $\frac{\partial f}{\partial t} = -\frac{1}{2}\|\nabla f\|^2$. We say the PDE *generates* the scale-space. It is PDEs such as these that PDE-G-CNNs employ.

In the first paragraph of the introduction we stated that in a PDE-CNN the trainable parameters are the coefficients that determine the effect of the used PDEs. However, the PDEs we have seen just now have no free coefficients, so what is there to train? The explanation is that we do not solely utilize the standard inner product on \mathbb{R}^2 ; rather, we consider general inner products $\langle x, y \rangle_G = x^T G y$, with $G \in \mathbb{R}^{2 \times 2}$ a symmetric positive definite matrix. When using different inner products, concepts such as Laplacian, gradient, and norm change accordingly, consequently altering the effect of the PDEs that depend on them. In concrete terms, this means that in the formulas (1), (2), and (3) the norm $\|x\|$ is changed to $\|x\|_G := \sqrt{x^T G x}$. It is this matrix G that is learned during training in the PDE-CNN framework.

In Figure 4 a quadratic dilation scale-space representation is visualized with a non-standard inner product. In the third picture of the first row of Figure 2b we can observe that the trained PDE-CNN has clearly learned to perform a vertically-oriented anisotropic dilation.

Scale-spaces are a natural choice for computer vision solutions (either neural networks or classical methods) as they respect the inherent symmetries of images, that being translation, rotational, and scaling symmetries. What we mean by this mathematically is that, for example, the scale-space g_t of a translated image $g_0 = T_v f_0$, is equal to the translated scale-space of the original image: $g_t = T_v f_t$. Here T_v is the translation

¹For a full treatment of viscosity solutions see [15].

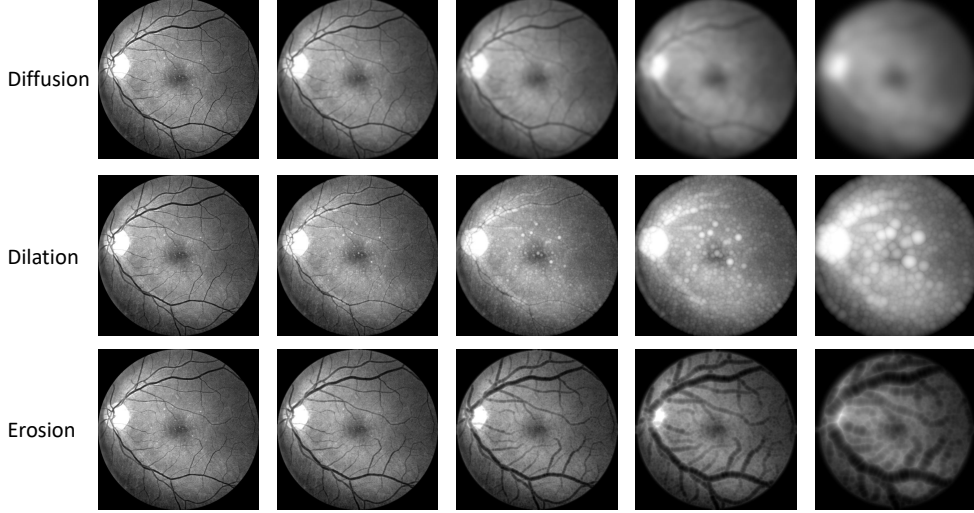


Fig. 3: The Gaussian, quadratic dilation, and quadratic erosion scale-space representations of a grayscale image of the fundus of the eye at various scale-parameters. In the Gaussian scale-space both white and black features fade away towards a uniform image. In the dilation scale-space the black details (low values), such as the vessels, vanish at bigger scales. In the erosion scale-space the white details (high values), such as the space between vessels, are removed at higher scales.

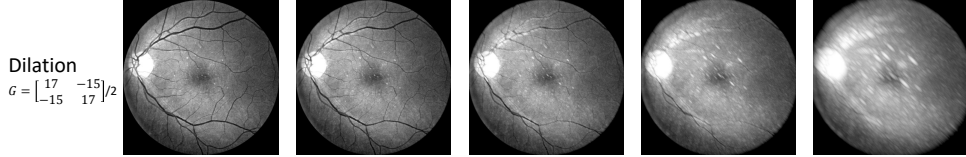


Fig. 4: The quadratic dilation scale-space representation with the (very) anisotropic inner product $G = \begin{bmatrix} 17 & -15 \\ -15 & 17 \end{bmatrix} / 2$. This can be compared with the dilation scale-space seen in Figure 3 that uses the standard isotropic inner product $G = I$. Such an anisotropic dilation can, for example, be used to remove unaligned vessels. This is best seen in the fourth image where only the diagonally oriented vessels are still apparent.

operator defined by $(T_v f)(x) = f(x - v)$. Analogous statements hold for the rotation and scaling symmetries. We say that creating the scale-space representation of an image is *equivariant* with respect to translation, rotations and scalings.

Neural networks that employ scale-spaces inherit these desirable properties, meaning that these architectures are translation, rotation, and scaling equivariant. Machine learning architectures that are inherently equivariant enjoy benefits such as data efficiency, reduced parameter count, and robustness [16, 17]. From the translation equivariance (and a form of linearity) it also follows that the architectures that employ scale-spaces are naturally convolution neural networks,

which are easy to implement and fast to evaluate due to the highly parallelizable nature of convolutional operations. In recent scale equivariant networks literature [18–21] the link to scale-space theory is also emphasized. In fact, the architectures they design are scale-spaces in the broad sense.

In this article (Section 4.1) we will formulate six axioms that a scale-space representation for a PDE layer should satisfy, and motivate each of them from a machine learning perspective.

In summary, to return to the question of why the diffusion, dilation, and erosion PDEs are employed in PDE-G-CNNs, the answer is

that these PDEs generate scale-spaces, and scale-spaces are a natural choice for computer vision solutions. However, this raises a follow-up question: **are there any other PDEs that generate scale-spaces?** To even start answering this question we need a proper mathematical definition of a scale-space, and this begins by explaining what we mean when we say a scale-space is *(quasi)linear*.

Creating Gaussian scale-spaces is linear in the sense that if one takes two images $f_0, g_0 : \mathbb{R}^2 \rightarrow \mathbb{R}$ and two scalars $a, b \in \mathbb{R}$, then the scale-space h_t of the image $h_0 = af_0 + bg_0$ is equal to $h_t = af_t + bg_t$. But, in an analogous manner, the quadratic dilation scale-space is *quasilinear* in the sense that the scale-space of the image $h_0 = \max\{a + f_0, b + g_0\}$, where we interpret the maximum pointwise, is equal to $h_t = \max\{a + f_t, b + g_t\}$. In the same way, the quadratic erosion scale-space is quasilinear in the min sense. One can quickly check these properties through their convolutional form as seen above. To define what we mean with quasilinear more generally we need to introduce the notion of a *semifield*.

A semifield $(R, 0, 1, \oplus, \otimes)$ is an algebraic structure like a field but where we relax the requirement that the addition \oplus has inverses. The prototypical example of a semifield are the non-negative real numbers $L_{\geq 0} = (\mathbb{R}_{\geq 0}, 0, 1, +, \times)$ with standard addition and multiplication. We have already seen two other examples of semifields in the dilating and eroding convolutions above. Namely, the *tropical* semifields $T_+ = (\mathbb{R} \cup \{-\infty\}, -\infty, 0, \max, +)$ and $T_- = (\mathbb{R} \cup \{\infty\}, \infty, 0, \min, +)$. In the tropical semifields the minimum(or maximum) of two numbers becomes semifield addition, and normal addition becomes semifield multiplication (which can be confusing).

With the definition of a semifield we can state the quasilinearity of a scale-space formally as *semifield R -linearity*. So, like before, consider a semifield R and two semifield-valued images $f_0, g_0 : \mathbb{R}^2 \rightarrow R$ and two elements $a, b \in R$. Then by a scale-space being R -linear we mean that the scale-space of the R -linear combination of images $h_0 = (a \otimes f_0) \oplus (b \otimes g_0)$ is equal to R -linear combination of scale-spaces $h_t = (a \otimes f_t) \oplus (b \otimes g_t)$. In other words, the operation that takes an image and returns its scale-space representation is a semifield linear operator. For example, the

Gaussian scale-space is $L_{\geq 0}$ -linear, the quadratic dilation scale-space is T_+ -linear, and the quadratic erosion scale-space is T_- -linear.

In [22, 23] it is argued in an axiomatic way that the only linear scale-space representations correspond to solutions of the fractional diffusion (pseudo-)PDE system on $\mathbb{R}^2 \times \mathbb{R}_{\geq 0}$:

$$\begin{aligned} \frac{\partial f}{\partial t} &= -\frac{1}{\alpha}(-\Delta)^{\alpha/2}f, \quad t \geq 0 \\ f(\cdot, 0) &= f_0, \end{aligned} \quad (4)$$

where $-(-\Delta)^{\alpha/2}$ is a (fractional) power of the *Laplacian*, and $\alpha > 0$. In a completely analogous manner, one can show [24, 25] that the only morphological scale-spaces, that being scale-spaces that are T_+ or T_- linear, correspond to (viscosity) solutions of the α -dilation and α -erosion PDE:

$$\begin{aligned} \frac{\partial f}{\partial t} &= \pm \frac{1}{\alpha} \|\nabla f\|^\alpha, \quad t \geq 0 \\ f(\cdot, 0) &= f_0, \end{aligned} \quad (5)$$

with $\alpha > 1$.

The scale-space representations that these α dependent PDEs generate can also written in terms of linear, dilating, and eroding convolutions, just as the special quadratic ($\alpha = 2$) cases seen in equations (1), (2) and (3). However, the kernels k_t in these cases are slightly more involved.

To give an example, the α -erosion scale-space representation is given by

$$f_t = k_t \boxminus f_0, \quad k_t(x) = \frac{t}{\beta} \left(\frac{\|x\|}{t} \right)^\beta,$$

with $1/\alpha + 1/\beta = 1$, and in Figure 5 the $\alpha = 8/7$ case is visualized. The $\alpha > 1$ parameter in this case regulates between “hard” min-pooling when α is close to 1, and “softer” min-pooling when α is bigger. In Figure 6 the kernel k_t is visualized for different values of α .

Now, to return to the question of whether there are any other PDEs that generate scale-spaces. One answer to the question is that, other than the α dependent PDEs (4) and (5), there exist no other PDEs that generate linear or morphological scale-spaces. This answer is unsatisfactory of course, as it does not consider the possibility of using semifields other than linear and tropical ones.

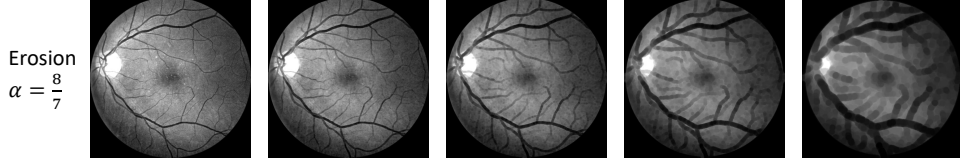


Fig. 5: The α -erosion scale-space representation with $\alpha = 8/7$. This can be compared with the quadratic ($\alpha = 2$) erosion scale-space seen in Figure 3. Notice that with smaller α the effect of the erosion becomes more abrupt and *bokeh*-like.

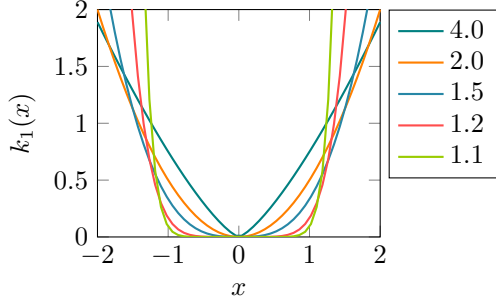


Fig. 6: The shape of the α -erosion scale-space kernel $k_t(x) = t(\|x\|/t)^\beta/\beta$ with $t = 1$ and various values of α , where we recall $1/\alpha + 1/\beta = 1$.

1.2 Contribution

We take the standard scale-space axioms but state them in terms of semifields. The result is a theory that encapsulates a large class of known scale-spaces. The goal of this generalization is to allow for the discovery (or invention) of new scale-spaces that can be used in the design of PDE-based neural networks.

We will only consider semifields that are commutative and one-dimensional, and the domain of the scale-spaces will be the two-dimensional Euclidean space \mathbb{R}^2 . To maintain a practical perspective, we will consistently connect the overarching theory using five example semifields: the linear, root, logarithmic, tropical min, and tropical max semifields.

From the axioms we show in Theorem 1 that every semifield corresponds to a unique family of semifield scale-spaces, this being the main theoretical result of the article. This shows that PDE-based neural networks, in their current form, can be extended greatly by adding scale-spaces that correspond to various currently unutilized semifields.

We experimentally assess how effective the incorporation of new semifields and their corresponding scale-spaces is in Section 6.3, and verify that PDE-CNNs exhibit superior data efficiency, reduced parameter count, and competitive performance compared to traditional CNNs in Section 6.2.

These results align with the conclusions in [1, 4–6] where PDE-G-CNNs and G-CNNs on the roto-translation group $G = \text{SE}(2)$ are compared.

1.3 Short Outline

In Section 2 we provide a non-exhaustive list of related literature. In Section 3 we define semifields and all related structures and operations. This is necessary to define the semifield scale-space axioms. In Section 4 we state the semifield scale-space axioms. In Section 5 we show that once a semifield is chosen a unique (one-parameter) family of scale-spaces arise. This main result is Theorem 1. In Section 6 we briefly note on the architectural design of PDE-CNNs in practice, and we lay out two experiments and discuss their results. In Section 7 we conclude the article.

2 Related Work on Scale Spaces

In this section we provide a noncomprehensive list of related scale-space literature in chronological order.

- In T. Iijima’s paper [11] the first [12] axiomatic treatment of linear scale-space theory is presented. Axioms such as linearity, translation and rotation equivariance, one-parameter semigroup property, and most notably, the scale equivariance, can all be found in Iijima’s article.
- In J.J. Koenderink’s article [13] the structure of images is analyzed through the Gaussian

scale-space representation generated by the Laplacian.

- R. Brockett and P. Maragos [14] were the first [26] to show that morphological operators like dilations and erosions in image processing can be described in terms of nonlinear Hamilton–Jacobi PDEs, whose Lax–Oleinik solutions [15] boil down to quasi-linear convolutions over the tropical semifield (even on Riemannian homogeneous spaces [27, 28]). For PDE-based neural networks this allows for equivariant max-pooling over Riemannian balls (making ReLU-activations obsolete) [1].
- In L. Alvarez, F. Guichard, P.L. Lions, and J.M. Morel [29] provide a very general axiomatic approach to PDE-based scale-spaces. The strength of this approach is that it also includes mean curvatures flows [30] as highly powerful non-linear PDEs (also on Lie groups [1, 31]). Solutions of such non-linear PDEs may be solved with median filtering [32], however, they lack semifield linearity (taking mean/median are not associative binary operations). This makes those PDEs unfortunately less tangible for PDE-based neural networks where a form of linearity is important, both theoretically [4] and from a parallel GPU-implementation point of view. We will not insist in using solely (local) differential operators in our evolution generators, and more importantly, we take semifield linearity as a (restrictive) axiom.
- In E. Pauwels, L. van Gool, P. Fiddelaers, and T. Moons [22] an extended class of linear scale-spaces is introduced. They basically see that (fractional) powers of the Laplacian are valid linear scale-space generators, but never state the actual (pseudo-)PDE. Nevertheless, their work elegantly points out the restrictiveness of the scale-space axioms, in particular the scale equivariance axiom. Analysis of the scale-space axioms in the Fourier domain is extensively used, an approach that we also use in this article in the more general semifield setting.
- In L. Dorst and R. van den Boomgaard [33] the slope transform is presented. The slope transform is shown to be the morphological counterpart of the Fourier transform, and related to the Legendre–Fenchel transform. In fact, the Legendre–Fenchel transform can already be seen as the morphological equivalent of the Fourier transform if one restricts to convex/concave functions. The semifield Fourier transform we introduce reduces to the Legendre–Fenchel transform in the tropical semifield cases.
- In L. Florack [34] nonlinear scale-spaces are obtained by performing a monotonic transformation (known as a “Cole–Hopf” transform [15, Ch.4.4]) on the grey-values of a standard linear scale-space and deducing what nonlinear PDE corresponds to the obtained evolution. This transformation neatly bridges linear, logarithmic, and in the extreme cases, morphological scale-spaces, and we will use this link extensively.
- In H. J. Heijmans and R. van den Boomgaard [26] a very general algebraic framework for scale-spaces is given. Importantly, their perspective is (initially) totally divorced from PDEs, convolutions, and kernels, and focuses solely on the operator family. We will define our semifield scale-spaces in the same manner: The word ‘PDE’ is not present in our axioms, the PDEs solely come from algebraic symmetry constraints.
- In M. Welk [24] “Generalised morphological scale-spaces” are explored which look a lot like semifield scale-spaces. φ -deformed addition is defined by pulling back the standard linear semifield structure using the mapping φ . Linear, logarithmic, root, and tropical semifields all make an appearance, together with their corresponding semifield integration and scale-spaces. In this article we will rely on those useful scale-space tools and provide a general axiomatic derivation via the semifield Fourier transform.
- In M. Felsberg and G. Sommer [35] the *Poisson scale-space* is introduced, a linear scale-space that only fails to meet Koenderink’s principle. They introduce a weaker form of the causality axiom, which they call *relaxed causality*, and show that the Poisson scale-space does satisfy this relaxed notion. The Poisson scale-space fits within the scale-spaces of Pauwels et al. [22]. A key aspect of the Poisson scale-space is that it allows for a 3D Clifford analytic extension useful for phase based image processing [35]. Our work

will remain in the scalar-valued setting (and not study flow-field extensions) but we do include Poisson scale-space as a valid member, as it arises by the operator factorisation: $\Delta + \partial_t^2 = (\partial_t - \sqrt{-\Delta})(\partial_t + \sqrt{-\Delta})$.

- In R. Duits, L. Florack, J. de Graaf, and B. ter Haar Romenij [36] the usual linear scale-space axioms are combined with extra axioms/properties such as *weak/strong causality* and *increase of entropy*. In the end the same conclusion as Pauwels et al. [22] is reached: fractional powers of the Laplacian $(-\Delta)^{\alpha/2}$ generate valid scale-spaces and this is a special case of Yosida's theory [37, ch:11] on strongly continuous one-parameter semigroups. The α -scale-spaces include Poisson ($\alpha = 1$) and Gaussian ($\alpha = 2$) scale-space, and coincides with the linear semifield scale-spaces we will axiomatically find in this article.
- In B. Burgeth and J. Weickert [38] the important connection between linear and morphological scale-spaces is illuminated using the Cramér transform. The Cramér transform gives us a way to translate between the kernels of the linear and morphological scale-spaces. We will show that the kernels of all scale-spaces have the same form in the Fourier domain (this being our main theorem), illuminating further why this isomorphism from the linear to the tropical semifield makes sense. This transform is also used in [39] relating *probability calculus* on the linear semifield, to *decision calculus* on the tropical semifield.
- In M. Schmidt and J. Weickert [25] morphological counterparts of linear scale-spaces are explored. The Cramér–Fourier transform is introduced. This work directly builds on the previous work of B. Burgeth and J. Weickert [38], and is a modification of the Cramér transform. The Cramér–Fourier transform, in contrast to the Cramér transform, allows for a generalization to groups other than \mathbb{R}^2 .

3 Semifield Theory

In this section we define semifields (Definition 1) and all mathematical structures and operations made from them. This includes important concepts such as semimodules (Definition 7), linearity

(Definition 8), measures (Definition 16), integration (Definition 18), convolution (Definition 20), and Fourier transforms (Definition 25).

3.1 Semifield, Semimodules & Linearity

Definition 1 (Semifield). A (commutative) semifield R is a tuple $R = (R, 0, 1, \oplus, \otimes)$ where $\oplus, \otimes : R \times R \rightarrow R$ are two commutative and associative binary operations on R called semifield addition and multiplication, such that for all $a, b, c \in R$:

$$\begin{aligned} a \oplus 0 &= a, \\ a \otimes 1 &= a, \\ a \neq 0 &: \exists a^{-1} : a \otimes a^{-1} = 1, \\ a \otimes 0 &= 0, \\ a \otimes (b \oplus c) &= (a \otimes b) \oplus (a \otimes c). \end{aligned}$$

In other words, a semifield is a field where we do not require to have “negative elements”, that being additive inverses.

Throughout the article we will denote an arbitrary semifield-related operation with a circled version of the most closely related linear counterpart. Some example symbols are \oplus , \otimes , \oint , and \circledast , which respectively correspond to semifield addition, multiplication, integration, and convolution.

In this article we mainly consider the following semifields:

Definition 2 (Semifields of Interest).

- The linear semifield $L = (\mathbb{R}, 0, 1, +, \times)$ with the usual addition $+$ and multiplication \times . We can restrict the set to $\mathbb{R}_{\geq 0}$ and we write $L_{\geq 0}$ in that case.
- The root semifields $R_p = (\mathbb{R}_{\geq 0}, 0, 1, \oplus_p, \times)$ with $p \neq 0$ where semifield addition is $a \oplus_p b := \sqrt[p]{a^p + b^p}$, and where semifield multiplication is normal multiplication.
- The logarithmic semifields $L_\mu = (\mathbb{R} \cup \{\pm\infty\}, \pm\infty, 0, \oplus_\mu, +)$ with $\mu \neq 0$ where semifield addition is $a \oplus_\mu b := \frac{1}{\mu} \ln(e^{\mu a} + e^{\mu b})$, and where semifield multiplication is normal addition. If $\mu > 0$ we add $-\infty$ to the ring to act as the additive identity, and if $\mu < 0$ we add $+\infty$.

- d) The tropical² max semifield $T_+ = (\mathbb{R} \cup \{-\infty\}, -\infty, 0, \max, +)$, where \max is semifield addition, and usual addition is semifield multiplication.
- e) The tropical min semifield $T_- = (\mathbb{R} \cup \{\infty\}, \infty, 0, \min, +)$, where \min is semifield addition, and usual addition is semifield multiplication.

The family of logarithmic semifields is interesting as in the limits one has:

$$\begin{aligned}\lim_{\mu \rightarrow +\infty} a \oplus_\mu b &= \max(a, b), \\ \lim_{\mu \rightarrow -\infty} a \oplus_\mu b &= \min(a, b).\end{aligned}$$

Thereby, the family of logarithmic semifields L_μ relate to the tropical semifields T_\pm in the extreme cases of μ .

Definition 3 (Semifield Isomorphism). Let $R = (R, 0, 1, \oplus, \otimes)$ and $\tilde{R} = (\tilde{R}, \tilde{0}, \tilde{1}, \tilde{\oplus}, \tilde{\otimes})$ be two semifields. A semifield isomorphism $\varphi : R \rightarrow \tilde{R}$ is a bijective mapping that satisfies for all $a, b \in R$:

$$\begin{aligned}\varphi(0) &= \tilde{0}, \\ \varphi(1) &= \tilde{1}, \\ \varphi(a \oplus b) &= \varphi(a) \tilde{\oplus} \varphi(b), \\ \varphi(a \otimes b) &= \varphi(a) \tilde{\otimes} \varphi(b).\end{aligned}$$

If there exists a semifield isomorphism between two semifields they are called isomorphic.

Proposition 1 (Some Semifields Isomorphism).

- The root semifields R_p are isomorphic to the nonnegative linear semifield $L_{\geq 0}$, with the isomorphism $\varphi_p : R_p \rightarrow L_{\geq 0}$ being $\varphi_p(x) = x^p$.
- The logarithmic semifields L_μ are isomorphic to the nonnegative linear semifield $L_{\geq 0}$, with the isomorphism $\varphi_\mu : L_\mu \rightarrow L_{\geq 0}$ being $\varphi_\mu(x) = e^{\mu x}$.
- The tropical max semifield T_+ is isomorphic to the tropical min semifield T_- , with the isomorphism $\varphi : T_+ \rightarrow T_-$ being $\varphi(x) = -x$.
- Informally, in the limit $\mu \rightarrow \pm\infty$ the logarithmic semifields L_μ “converge” to the tropical semifields T_\pm .

The above proposition shows that although we defined five semifields of interest, as listed in Definition 2, we are, in fact, only working with 2 non-isomorphic ones.

For the purpose of analysis we endow the semifields with a metric. Normally, a linear structure X is endowed with a norm $\|\cdot\| : X \rightarrow \mathbb{R}_{\geq 0}$ and afterwards a metric d is defined through $d(a, b) = \|a - b\|$. This is not possible in our semifield setting as we do not necessarily have additive inverses (consider for example the tropical semifields).

Definition 4 (Semifield Metric). Let R be a semifield. A semifield metric $\rho : R \times R \rightarrow \mathbb{R}_{\geq 0}$ is a metric such that for all $a, b, c \in R$ we have:

$$\begin{aligned}\rho(c \oplus a, c \oplus b) &\leq \rho(a, b), \\ \rho(c \otimes a, c \otimes b) &= \rho(c, 0)\rho(a, b).\end{aligned}$$

These properties are direct generalizations of the common notions of translation invariance and absolute homogeneity. More importantly, they ensure that semifield addition \oplus and multiplication \otimes are continuous (w.r.t the metric).

Definition 5 (Employed Semifield Metrics).

- a) In the linear semifield L case we use the metric $\rho_L(a, b) = |a - b|$.
- b) In the root semifields R_p case we use the metric $\rho_{R_p}(a, b) = |a^p - b^p|$.
- c) In the logarithmic semifields L_μ case we use the metric $\rho_{L_\mu}(a, b) = |e^{\mu a} - e^{\mu b}|$ ³.
- d) In the tropical max semifield T_+ case we use the metric $\rho_{T_+}(a, b) = |e^a - e^b|$.
- e) In the tropical min semifield T_- case we use the metric $\rho_{T_-}(a, b) = |e^{-a} - e^{-b}|$.

The root and logarithmic semifield metrics are natural as they borrow the metric on the linear semifield L through the isomorphisms $\varphi_p(x) = x^p$ and $\varphi_\mu(x) = e^{\mu x}$, see Proposition 1. Similarly, the tropical min and max semifield metrics relate by their isomorphism $\varphi(x) = -x$.

Definition 6 (One-Dimensional Semifield). Let R be a metric semifield. If R as a topological space (with the topology induced by the metric) is locally homeomorphic to one-dimensional Euclidean space we say it is one-dimensional.

Just as mathematical rings and fields can be used to create modules and vector spaces, we

²Coined in honor of the Hungarian-born Brazilian computer scientist Imre Simon [40].

³We define $e^{-\infty} = 0$.

define an analogous structure called a semimodule using semifields.

Definition 7 (Semimodule). Let $R = (R, \mathbb{0}, \mathbb{1}, \oplus, \otimes)$ be a semifield. A R -semimodule $V = (V, \oplus_V, \otimes_V, \mathbb{0}_V)$ over R is a set with a commutative and associative binary operation $\oplus_V : V \times V \rightarrow V$ called addition, and another binary operation $\otimes_V : R \times V \rightarrow V$ called (left) scalar multiplication, such that for all $a, b \in R$ and $u, v \in V$:

$$\begin{aligned} v \oplus_V \mathbb{0}_V &= v, \\ \mathbb{1} \otimes_V v &= v, \\ \mathbb{0} \otimes_V v &= \mathbb{0}_V, \\ (a \oplus b) \otimes_V v &= (a \otimes_V v) \oplus_V (b \otimes_V v), \\ a \otimes_V (u \oplus_V v) &= (a \otimes_V u) \oplus_V (a \otimes_V v). \end{aligned}$$

We do not write the subscript V on the operations of a semimodule V from here on out, as is usual.

Now that we have semimodules we can speak of semifield-linearity in its full generality. The notion of semifield-linearity is totally analogous to the normal notion of linearity, therefore the name.

Definition 8 (Semifield Linear). Let V_1, V_2 be two semimodules over the same semifield R . A mapping $\varphi : V_1 \rightarrow V_2$ is called R -linear if for all $a, b \in R$ and $u, v \in V_1$ we have:

$$\varphi(a \otimes u \oplus b \otimes v) = a \otimes \varphi(u) \oplus b \otimes \varphi(v).$$

3.2 Functions, Measurability & Integration

The prototypical semimodule over a semifield is the space of all semifield-valued functions on a set.

Definition 9 (Function Semimodule). Let R be a semifield. Consider the set $F(\mathbb{R}^2, R)$ of all R -valued functions $f : \mathbb{R}^2 \rightarrow R$. The set $F(\mathbb{R}^2, R)$ forms a R -semimodule under point-wise semifield addition and multiplication. The semimodule $F(\mathbb{R}^2, R)$ is called the function semimodule over \mathbb{R}^2 . More generally, any subsemimodule of $F(\mathbb{R}^2, R)$ is also called a function semimodule over \mathbb{R}^2 .

On the function semimodule $F(\mathbb{R}^2, R)$ we define the following natural R -linear domain transformation operators:

Definition 10 (Operators on Function Semimodule).

- **Translation Operator:** For all translation vectors $v \in \mathbb{R}^2$ we define the translation operator \mathcal{T}_v

$$(\mathcal{T}_v f)(x) := f(-v + x). \quad (6)$$

- **Rotoreflexion Operator:** For all orthonormal matrices $Q \in \mathbb{R}^{2 \times 2}$ we define the rotoreflexion operator \mathcal{R}_Q

$$(\mathcal{R}_Q f)(x) := f(Q^{-1}x). \quad (7)$$

- **Scaling Operator:** For all scalings $s \in \mathbb{R}_{>0}$ we define the scaling operator \mathcal{S}_s

$$(\mathcal{S}_s f)(x) := f\left(\frac{x}{s}\right). \quad (8)$$

- **Pointwise Operator:** For all φ we define the pointwise operator \mathcal{P}_φ

$$(\mathcal{P}_\varphi(f))(x) := \varphi(f(x)). \quad (9)$$

To avoid pathological cases, we introduce standard measure theoretical concepts.

Definition 11 (Measurable Space & Set). Let (X, d) be a complete metric space. We equip the space X with the natural Borel sigma-algebra B induced by the metric d . This turns X into a measurable space. A measurable set is any element of the Borel sigma algebra B .

With the above definition we can turn both \mathbb{R}^2 and any metric semifield R into a measurable space.

Definition 12 (Measurable Function). Let R be a metric semifield and $f : \mathbb{R}^2 \rightarrow R$ a function. The function f is called a measurable function if the pre-image of any measurable set is a measurable set.

The set of measurable functions is broad enough to be well-behaved under pointwise limits, as the following lemma describes.

Lemma 1. *Let R be a metric semifield, and let $f(x) = \lim_{n \rightarrow \infty} f_n(x)$ be the pointwise limit of measurable functions $f_n : \mathbb{R}^2 \rightarrow R$. Then f is also measurable.*

A proof of a generalization of this lemma can be found at [41]. But there exists an even stronger statement that describes measurable functions as

pointwise limits of indicator functions simple functions, which are made from indicator functions.

Definition 13 (Indicator Function). Let R be a semifield and $A \subseteq \mathbb{R}^2$ any set. We define the indicator function $\mathbb{1}_A$ of A as:

$$\mathbb{1}_A(x) = \begin{cases} \mathbb{1} & \text{if } x \in A \\ 0 & \text{otherwise} \end{cases}$$

Definition 14 (Simple Function). Let R be a semifield. A simple function $s : \mathbb{R}^2 \rightarrow R$ is a finite R -linear combination of indicator functions of measurable sets A_i .

$$s = \bigoplus_{i=1}^n a_i \otimes \mathbb{1}_{A_i},$$

where each $a_i \in R$.

The link between measurable and simple functions is as follows.

Lemma 2. *Let R be a metric semifield and consider semifield-valued functions on \mathbb{R}^2 . The pointwise limit of a sequence of simple functions is measurable. Every measurable function is the pointwise limit of a sequence of simple functions.*

Proof. The pointwise limit of a sequence of simple functions being measurable follows immediately from Lemma 1, as simple functions are measurable. Showing that every measurable function is the pointwise limit of simple functions goes via a straightforward construction. \square

For every semifield there is a natural associated class of functions. We would like to specify this class in an axiomatic sense. This is where the sum-approachable definition comes into play. It is a restriction of the well-known statement that “every measurable function is the limit of simple functions”.

Definition 15 (Sum-Approachable). Let R be a metric semifield. A function $f : \mathbb{R}^2 \rightarrow R$ is sum-approachable if there exists $a_i \in R$ and $A_i \subseteq \mathbb{R}^2$ open such that we have

$$f(x) = \lim_{n \rightarrow \infty} \bigoplus_{i=1}^n a_i \otimes \mathbb{1}_{A_i}(x).$$

The semimodule of all sum-approachable functions $f : \mathbb{R}^2 \rightarrow R$ is denoted by $S(\mathbb{R}^2, R)$.

There are two differences between sum-approachable and measurable: we only consider open sets, not measurable sets, and we have a limit of a semifield sum of indicator functions, not just a limit.

A function being sum-approachable is more restrictive than one might think at first sight. The following lemma illustrates this by showing that in the tropical cases the sum-approachable functions enjoy the property of being semicontinuous, something that does *not* happen in the linear case.

Lemma 3. *A sum-approachable function $f : \mathbb{R}^2 \rightarrow T_+$ is lower semicontinuous. A sum-approachable function $f : \mathbb{R}^2 \rightarrow T_-$ is upper semicontinuous.*

Proof. Consider the tropical max semifield case for the moment. Every indicator function $\mathbb{1}_A(x)$ with $A_i \subseteq \mathbb{R}^2$ open is lower semicontinuous in this case. The limit-semifield-sum in the definition of sum-approachable turns into a pointwise supremum in this case. The pointwise supremum of lower semicontinuous functions is again lower semicontinuous⁴. Thus, every sum-approachable function $f : \mathbb{R}^2 \rightarrow T_+$ is lower semicontinuous. *Mutatis mutandis*, the exact same argument holds in the tropical min semifield case. \square

Definition 16 (Semifield Measure). Let Σ be the Borel sigma algebra on \mathbb{R}^2 and $R = (R, 0, \mathbb{1}, \oplus, \otimes)$ a semifield. A semifield measure $\mu : \Sigma \rightarrow R$ is a mapping that satisfies the following properties.

- **Nullity of Empty Set:**

$$\mu(\emptyset) = 0.$$

- **Disjoint Additivity:** For all disjoint sets $A, B \in \Sigma$:

$$\mu(A \cup B) = \mu(A) \oplus \mu(B),$$

which we extend to countable collections of pairwise disjoint sets.

⁴Let $f(x) = \sup_n f_n(x)$. Let $\varepsilon > 0$ and $x_0 \in \mathbb{R}^2$. Choose N such that $f_N(x_0) > f(x_0) - \varepsilon/2$. Choose $\delta > 0$ such that $f_N(x) > f_N(x_0) - \varepsilon/2$ when $|x - x_0| < \delta$. Then $f(x) > f_N(x) > f_N(x_0) - \varepsilon/2 > f(x_0) - \varepsilon$ [42].

- **Unity of Unit Square:**

$$\mu([0, 1]^2) = \mathbb{1}.$$

- **Translation Invariance:** For all $A \in \Sigma$ and $v \in \mathbb{R}^2$:

$$\mu(A + v) = \mu(A).$$

- **Rotoreflexion Invariance:** For all $A \in \Sigma$ and all orthonormal matrices $Q \in \mathbb{R}^{2 \times 2}$:

$$\mu(QA) = \mu(A).$$

- **Scaling Equivariance:** There exist a group homomorphism $\chi : (\mathbb{R}_{>0}, \times) \rightarrow (R \setminus \{0\}, \otimes)$ such that for all scalings $s \in \mathbb{R}_{>0}$ and all $A \in \Sigma$:

$$\mu(sA) = \chi(s) \otimes \mu(A).$$

Definition 17 (Employed Semifield Measure).

- In the linear semifield L case we use standard Lebesgue measure λ . $\mu_L(A) = \lambda(A)$. The scaling factor is $\chi(s) = s^2$.
- In the root semifields R_p cases we use $\mu_{R_p}(A) = \sqrt[p]{\lambda(A)}$. The scaling factor is $\chi(s) = \sqrt[p]{s^2}$.
- In the logarithmic semifields L_μ cases we use $\mu_{L_\mu}(A) = \frac{1}{\mu} \ln \lambda(A)$. The scaling factor is $\chi(s) = \frac{1}{\mu} \ln s^2$.
- In the tropical max semifield T_+ case we use $\mu_{T_+}(A) = 0^5$. The scaling factor is $\chi(s) = 0$.
- In the tropical min semifield T_- case we use $\mu_{T_-}(A) = 0$. The scaling factor is $\chi(s) = 0$.

Definition 18 (Semifield Integration). Let R be a metric semifield, $S = S(\mathbb{R}^2, R)$ the space of sum-approachable functions, and μ a semifield measure. Let $\oint : (\text{dom}(\oint) \subset S) \rightarrow R$ be a functional with the following properties.

- **Semifield Linearity:** For all $a, b \in R$ and $f, g \in \text{dom}(\oint)$

$$\oint a \otimes f \oplus b \otimes g = a \otimes \left(\oint f \right) \oplus b \otimes \left(\oint g \right). \quad (10)$$

⁵Remember that the semifield one $\mathbb{1}$ in the tropical max semifield T_+ case is 0 (Definition 2).

- **Indicator Function:** For all measurable sets $A \subseteq \mathbb{R}^2$ we have

$$\oint \mathbb{1}_A = \mu(A). \quad (11)$$

- **Translation Invariance:** For all $v \in \mathbb{R}^2$ and $f \in \text{dom}(\oint)$

$$\oint \mathcal{T}_v f = \oint f. \quad (12)$$

- **Rotoreflexion Invariance:** For all orthonormal matrices $Q \in \mathbb{R}^{2 \times 2}$ and $f \in \text{dom}(\oint)$:

$$\oint \mathcal{R}_Q f = \oint f. \quad (13)$$

- **Scaling Equivariance:** For all scalings $s \in \mathbb{R}_{>0}$ and $f \in \text{dom}(\oint)$:

$$\oint \mathcal{S}_s f = \chi(s) \otimes \oint f, \quad (14)$$

where $\chi(s)$ is the scaling of the semifield measure \oint (Definition 16).

- **Fubini:** For all $f : \mathbb{R}^2 \times \mathbb{R}^2 \rightarrow R$ with both $f(\cdot, y), f(x, \cdot) \in \text{dom}(\oint)$, if one of the following integrals exists then they are equal:

$$\oint_y \oint_x f(x, y) = \oint_x \oint_y f(x, y). \quad (15)$$

We say such a functional is a semifield integration. A function f that is in the domain of the semifield integration is called integrable.

To emphasize over what slot we are integrating we may also write $\oint_{x \in \mathbb{R}^2} f(x) = \oint f$. To emphasize over what semifield R the integration is taking place we may also write $\oint = \oint^R$.

The first two properties of the semifield integration essentially nail down what the integration has to be. That is, for every simple function $s(x) = \bigoplus_{i=1}^n a_i \otimes \mathbb{1}_{A_i}(x)$ we have

$$\oint s = \bigoplus_{i=1}^n a_i \otimes \mu(A_i)$$

by semifield linearity. This then extends naturally to sum-approachable functions $f(x) =$

$\lim_{n \rightarrow \infty} \bigoplus_{i=1}^n a_i \otimes \mathbb{1}_{A_i}(x)$ by defining (with some caveats)

$$\oint f = \lim_{n \rightarrow \infty} \bigoplus_{i=1}^n a_i \otimes \mu(A_i).$$

The caveats here being that we need requirements on the exact nature of the sequence of simple functions for the above to be well-defined. To not get bogged down into the details we will just state what integration we will use for our relevant semifields, together with their domain of definition. In the case of the tropical semifields we show in Appendix B that the upcoming semifield integration is indeed the correct one.

Definition 19 (Employed Semifield Integration).

- a) In the linear semifield L case we use standard Lebesgue integration

$$\oint^L f = \int_{x \in \mathbb{R}^2} f(x) \, dx.$$

The domain $\text{dom}(\oint^L)$ is the space of Lebesgue integrable functions.

- b) In the root semifields R_p cases we use

$$\oint^{R_p} f = \sqrt[p]{\int_{x \in \mathbb{R}^2} f(x)^p \, dx}.$$

The domain $\text{dom}(\oint^{R_p})$ consist of all functions f such that f^p is Lebesgue integrable.

- c) In the logarithmic semifields L_μ cases we use

$$\oint^{L_\mu} f = \frac{1}{\mu} \ln \int_{x \in \mathbb{R}^2} e^{\mu f(x)} \, dx.$$

The domain $\text{dom}(\oint^{L_\mu})$ consist of all functions f such that $e^{\mu f}$ is Lebesgue integrable.

- d) In the tropical max semifield T_+ case we use the supremum \sup .

$$\oint^{T_+} f = \sup_{x \in \mathbb{R}^2} f(x).$$

The domain $\text{dom}(\oint^{T_+})$ consist of all functions f that are bounded from above.

- e) In the tropical min semifield T_- case we use the infimum \inf .

$$\oint^{T_-} f = \inf_{x \in \mathbb{R}^2} f(x).$$

The domain $\text{dom}(\oint^{T_-})$ consist of all functions f that are bounded from below.

The logarithmic and root semifield integration is natural as these semifields are isomorphic to the linear semifield, see Proposition 1. Additionally, the tropical max and min semifield integration are related through their isomorphism $\varphi(x) = -x$. Indeed, one has $\sup_{s \in S} s = -\inf_{s \in S} \{-s\}$.

Definition 20 (Semifield Convolution). Let R be a metric semifield. We define the semifield convolution \otimes of two integrable functions $f, g \in \text{dom}(\oint)$ as the new function $f \otimes g \in \text{dom}(\oint)$:

$$(f \otimes g)(x) := \oint_{y \in \mathbb{R}^2} f(x-y) \otimes g(y).$$

Showing that $f \otimes g$ is indeed in $\text{dom}(\oint)$ is an immediate consequence of the Fubini property of semifield integration (15). Moreover, the Fubini property gives us that the semifield convolution is associative:

$$f \otimes (g \otimes h) = (f \otimes g) \otimes h, \quad (16)$$

and the translation invariance of semifield integration together with the commutativity of the semifield multiplication gives us that the semifield convolution is commutative.

We want to perform some analysis in our function spaces, so we need a (pseudo)metric $\delta : S(\mathbb{R}^2, R) \times S(\mathbb{R}^2, R) \rightarrow \mathbb{R}_{\geq 0}$ (possibly with a restricted domain). Similarly as before, when we introduced a metric on the semifields, we can not make due with a norm on the function space as we have no additive inverses to turn the norm into a metric.

Definition 21 (Function Pseudometric). Let R be a semifield with metric ρ and $S = S(\mathbb{R}^2, R)$ the space of sum-approachable functions. A function (pseudo)metric $\delta : S \times S \rightarrow \mathbb{R}_{\geq 0} \cup \{\infty\}$ is a (pseudo)metric such that for all $f, g, h \in S$ and $a \in R$ we have:

$$\delta(h \oplus f, h \oplus g) \leq \delta(f, g),$$

$$\delta(a \otimes f, a \otimes g) = \rho(a, 0)\delta(f, g).$$

We allow for the (pseudo)metric to return ∞ .

Again, just as in Definition 4, these properties are generalizations of the common notions of translation invariance and absolute homogeneity, and they ensure that both function addition $\oplus : S \times S \rightarrow S$ and function scalar multiplication $\otimes : R \times S \rightarrow S$ are continuous (in both slots).

Definition 22 (Employed Function Pseudo-metric).

a) In the linear semifield L case we use

$$\delta_L(f, g) = \sqrt{\int_{\mathbb{R}^2} |f(x) - g(x)|^2 dx}.$$

b) In the root semifield R_p case we use

$$\delta_{R_p}(f, g) = \sqrt{\int_{\mathbb{R}^2} |f(x)^p - g(x)^p|^2 dx}.$$

c) In the logarithmic semifields L_μ case we use

$$\delta_{L_\mu}(f, g) = \sqrt{\int_{\mathbb{R}^2} |e^{\mu f(x)} - e^{\mu g(x)}|^2 dx}.$$

d) In the tropical max semifield T_+ case we use

$$\delta_{T_+}(f, g) = \sup_{x \in \mathbb{R}^2} |e^{f(x)} - e^{g(x)}|.$$

e) In the tropical min semifield T_- case we use

$$\delta_{T_-}(f, g) = \sup_{x \in \mathbb{R}^2} |e^{-f(x)} - e^{-g(x)}|.$$

Using the function (pseudo)metric we can make an appropriate function space:

Definition 23 (Metric Function Space). Let R be a metric semifield, $S = S(\mathbb{R}^2, R)$ the space of sum-approachable functions, and $\delta : S \times S \rightarrow \mathbb{R}_{\geq 0} \cup \{\infty\}$ a function (pseudo)metric. The function (pseudo)metric space $H = H(\mathbb{R}^2, R, \delta)$ is defined as

$$H := \{f \in S \mid \delta(0, f) < \infty\}.$$

To turn it into an actual metric space we need to identify elements using the following natural

equivalence relation \sim .

$$f \sim g \iff \delta(f, g) = 0.$$

This function space will be denoted with $\mathcal{H} = H/\sim$.

Definition 24 (Employed Function Spaces).

a) In the linear semifield L case we have

$$\mathcal{H}_L = \mathbb{L}^2(\mathbb{R}^2).$$

b) In the root semifield R_p case we have

$$\mathcal{H}_{R_p} = \{f : \mathbb{R}^2 \rightarrow R_p \mid e^{\mu f} \in \mathbb{L}^2(\mathbb{R}^2)\}.$$

c) In the logarithmic semifield L_μ case we have

$$\mathcal{H}_{L_\mu} = \{f : \mathbb{R}^2 \rightarrow L_\mu \mid f^p \in \mathbb{L}^2(\mathbb{R}^2)\}.$$

d) In the tropical max semifield T_+ case we have

$$\mathcal{H}_{T_+} = \{f : \mathbb{R}^2 \rightarrow T_+ \text{ l.s.c and b.f.a. }\},$$

where l.s.c means lower semicontinuous and b.f.a means bounded from above.

e) In the tropical min semifield T_- case we have

$$\mathcal{H}_{T_-} = \{f : \mathbb{R}^2 \rightarrow T_- \text{ u.s.c. and b.f.b. }\},$$

where u.s.c means upper semicontinuous and b.f.b means bounded from below.

3.3 Fourier Transform

We assume the existence of an injective Fourier transform that need only work on a very restricted class of semifield integrable functions.

Definition 25 (Semifield Fourier Transform). Let R be a metric semifield. A semifield Fourier Transform $\mathcal{F}_R : (\text{dom}(\mathcal{F}_R) \subseteq \text{dom}(\mathcal{F})) \rightarrow \text{dom}(\mathcal{F})$ is an operator satisfying (where we drop the subscript R for conciseness):

- **Semifield Linearity:** For all $a, b \in R$ and $f, g \in \text{dom}(\mathcal{F})$

$$\mathcal{F}(a \otimes f \oplus b \otimes g) = a \otimes (\mathcal{F}f) \oplus b \otimes (\mathcal{F}g).$$

- **Convolution Property:** For all $f, g \in \text{dom}(\mathcal{F})$ with $f \otimes g \in \text{dom}(\mathcal{F})$

$$\mathcal{F}(f \otimes g) = (\mathcal{F}f) \otimes (\mathcal{F}g). \quad (17)$$

- **Rotoreflexion Equivariance:** For all orthonormal matrices $Q \in \mathbb{R}^{2 \times 2}$

$$\mathcal{F} \circ \mathcal{R}_Q = \mathcal{R}_{Q^{-T}} \circ \mathcal{F}. \quad (18)$$

- **Scaling Equivariance:** For all scalings $s \in \mathbb{R}_{>0}$:

$$\mathcal{F} \circ \mathcal{S}_s = \chi(s) \otimes \mathcal{S}_{1/s} \circ \mathcal{F}, \quad (19)$$

where $\chi(s)$ is the scaling of the semifield measure (Definition 16).

- **Invertibility:** The domain $\text{dom}(\mathcal{F})$ is chosen such that the transform is injective and thus invertible on its image.

In the next definition we will specify the choice of semifield Fourier transform together with its appropriate choice of domain for all the semifields we consider (Definition 2). The choices we make here are sometimes more restrictive than strictly needed, but, as we will see in Section 5.2, we only need to be able to take the semifield Fourier transform of a very “small” set of functions.

Definition 26 (Employed Semifield Fourier Transform).

- a) In the linear semifield L case we use

$$(\mathcal{F}_L f)(\omega) = \int_{\mathbb{R}^2} f(x) e^{-i\omega \cdot x} dx.$$

The domain $\text{dom}(\mathcal{F}_L)$ is chosen to be the space of even, continuous, and absolutely integrable functions, with absolutely integrable Fourier transform. The inverse on its image is

$$(\mathcal{F}_L^{-1} \hat{f})(x) = \frac{1}{(2\pi)^2} \int_{\mathbb{R}^2} \hat{f}(\omega) e^{i\omega \cdot x} d\omega.$$

- b) In the root semifield R_p case we use

$$(\mathcal{F}_{R_p} f)(\omega) = \sqrt[p]{\int_{\mathbb{R}^2} f(x)^p e^{-i\omega \cdot x} dx}.$$

The domain $\text{dom}(\mathcal{F}_{R_p})$ is chosen such that f^p is in the domain of the linear Fourier transform $\text{dom}(\mathcal{F}_L)$, together with the restriction that the input of the p 'th root is nonnegative. The inverse on its image is

$$(\mathcal{F}_{R_p}^{-1} \hat{f})(x) = \sqrt[p]{\frac{1}{(2\pi)^2} \int_{\mathbb{R}^2} \hat{f}(\omega)^p e^{i\omega \cdot x} d\omega}.$$

- c) In the logarithmic semifield L_μ case we use

$$(\mathcal{F}_{L_\mu} f)(\omega) = \frac{1}{\mu} \ln \int_{x \in \mathbb{R}^2} e^{\mu f(x)} e^{-i\omega \cdot x} dx.$$

The domain $\text{dom}(\mathcal{F}_{L_\mu})$ is chosen such that $e^{\mu f}$ is in the domain of the linear Fourier transform $\text{dom}(\mathcal{F}_L)$, together with the restriction that the input of the natural logarithm is positive. The inverse on its image is

$$(\mathcal{F}_{L_\mu}^{-1} \hat{f})(x) = \frac{1}{\mu} \ln \left(\frac{1}{(2\pi)^2} \int_{\mathbb{R}^2} e^{\mu \hat{f}(\omega)} e^{i\omega \cdot x} d\omega \right).$$

- d) In the tropical max semifield T_+ case we use

$$(\mathcal{F}_{T_+} f)(\omega) = \sup_{x \in \mathbb{R}^2} f(x) - \omega \cdot x.$$

The domain $\text{dom}(\mathcal{F}_{T_+})$ is chosen to be space of even, continuous, concave, superlinear functions. The inverse on its image is

$$(\mathcal{F}_{T_+}^{-1} \hat{f})(x) = \inf_{\omega \in \mathbb{R}^2} \hat{f}(\omega) + \omega \cdot x.$$

- e) In the tropical min semifield T_- case we use

$$(\mathcal{F}_{T_-} f)(\omega) = \inf_{x \in \mathbb{R}^2} f(x) - \omega \cdot x.$$

The domain $\text{dom}(\mathcal{F}_{T_-})$ is chosen to be space of even, continuous, convex, superlinear functions. The inverse on its image is

$$(\mathcal{F}_{T_-}^{-1} \hat{f})(x) = \sup_{\omega \in \mathbb{R}^2} \hat{f}(\omega) + \omega \cdot x.$$

A proof that these transforms satisfy the definition can be found in Appendix A.

Remark 1. The Laplace-like transform

$$(\mathcal{L} f)(\omega) = \int_{\mathbb{R}^2} f(x) e^{-\omega \cdot x} dx$$

also satisfies Definition 25. However, and this is also mentioned in [25], this transform is limited in its applicability because it is only finitely-valued for functions with super-exponential decay⁶. Given these limitations of this transform, we instead use the normal Fourier transform.

⁶This Laplace transform is two-sided thus resulting in this extreme condition. Also, we do not regard the transform as a conditionally convergent improper integral.

Remark 2. The above semifield Fourier transforms typically relate to transforms of the type

$$(\mathcal{F}f)(\omega) = \oint f(x) \otimes \chi_\omega(x),$$

where χ_ω is an irreducible semifield-linear representation of \mathbb{R}^2 , but we choose to express them in common Fourier/Fenchel transforms to keep a clear track of function space restrictions.

Even though we have used complex numbers in the Fourier transforms, the resulting transformed functions are always of the proper form $\mathbb{R}^2 \rightarrow R$ due the domain consisting of even functions. This means that we could have freely replaced the $e^{-i\omega \cdot x}$ with $\cos(\omega \cdot x)$. In other words, we could have instead used the *Fourier cosine transform*.

4 Semifield Scale-space

In this section we will state and shortly discuss the semifield scale-space axioms, consider some examples semifield scale-spaces, and define what we mean with isomorphic scale-spaces.

4.1 Axioms

In [22] it is stated that “The only really nontrivial (and possibly too restrictive) assumption imposed on the scale-space operators, is that of linearity.”. By generalizing to semifield linearity we sidestep this restrictive assumption, without making the theory too abstract to be practically useful.

Let us shortly motivate the semifield scale-space axioms from a machine-learning perspective (building upon similar findings in mathematical deep learning [18–21]). The semifield linearity (Axiom 1) together with the translation equivariance (Axiom 5) will induce semifield convolutions that allow for fast parallel computations. The one-parameter semigroup property (Axiom 2) together with the strong continuity (Axiom 3) provides consistency and stability over evolution time. The one-parameter semigroup property (Axiom 2) together with the scaling equivariance (Axiom 4) allows us to constrain ourselves to a fixed end-time in a PDE sublayer, say $t = 1$, without loss of generality, further reducing the total parameter count. The scaling, translation, and roto-reflection equivariance (Axioms 4, 5 and 6) of the scale-space allows for the design of inherently equivariant networks, resulting in an architecture that is robust and data-efficient [16, 17].

Definition 27 (Semifield Scale-space). Let R be a one-dimensional metric semifield (Definition 6), $\mathcal{H} = \mathcal{H}(\mathbb{R}^2, R, \delta)$ a corresponding function semimodule (Definition 23), and $\Phi_t : \mathcal{H} \rightarrow \mathcal{H}$ be a family of operators, indexed by $t \geq 0$. We call Φ_t a semifield scale-space if it satisfies the following axioms:

1. **Semifield Linearity and Integral Operator:** We require that Φ is R -linear, that is for all $f, g \in \mathcal{H}$ and $a, b \in R$:

$$\Phi_t(a \otimes f \oplus b \otimes g) = a \otimes (\Phi_t f) \oplus b \otimes (\Phi_t g).$$

More specifically, we will assume for positive time $t > 0$ that Φ_t can be written as an integral operator:

$$(\Phi_t f)(x) = \oint_{y \in \mathbb{R}^2} \kappa_t(x, y) \otimes f(y),$$

for some kernel $\kappa_t : \mathbb{R}^2 \times \mathbb{R}^2 \rightarrow R$ with $\kappa_t(x, \cdot)$ within the domain of the semifield Fourier transform \mathcal{F}_R (Definition 25).

2. **One-Parameter Semigroup:** We require that Φ_t forms a one-parameter semigroup, that is for all $t, s \geq 0$:

$$\Phi_t \circ \Phi_s = \Phi_{t+s} \text{ and } \Phi_0 = \text{id},$$

where id is the identity map on \mathcal{H} .

3. **Strong Continuity:** We require that $\Phi_t f$ is continuous w.r.t. time t at any $t_0 > 0$ for all $f \in \mathcal{H}$:

$$\lim_{t \rightarrow t_0} (\Phi_t f) = \Phi_{t_0} f.$$

4. **Scaling Equivariance:** There exists a “scaling power” $\alpha > 0$ such that for all scalings $s > 0$ and all times $t \geq 0$:

$$\Phi_t \circ \mathcal{S}_s = \mathcal{S}_s \circ \Phi_{t/s^\alpha},$$

where \mathcal{S}_s is the scaling operator (8).

5. **Translation Equivariance:** We require that Φ commutes with all translations $v \in \mathbb{R}^2$:

$$\Phi_t \circ \mathcal{T}_v = \mathcal{T}_v \circ \Phi_t,$$

where \mathcal{T}_v is the translation operator (6).

6. **Rotoreflexion Equivariance:** We require that Φ commutes with all orthonormal matrices $Q \in \mathbb{R}^{2 \times 2}$:

$$\Phi_t \circ \mathcal{R}_Q = \mathcal{R}_Q \circ \Phi_t,$$

where \mathcal{R}_Q is the rotoreflexion operator (7).

In the linear semifield L case the linearity axiom in some sense already implies the integral operator axiom. The precise statement is known as the Schwartz kernel theorem, a main result in the theory of generalized functions/distributions. In the tropical semifield case a similar statement can be made, as demonstrated in [43, Thm.2.1]. But for other semifields such a statement can not be made just yet. For simplicity, and to be on the safe side, we therefor assume the integral operator axiom.

The one-parameter semigroup property is a natural axiom in the sense that it implies that the (infinitesimal) evolution “looks the same” at all times t . More precisely, the (strongly continuous) one-parameter semigroup property relates to the existence of a single generator that encapsulates the whole operator family. To understand, consider the linear semifield case, some initial $f_0 \in \mathcal{H}$, and its evolution $f_t := \Phi_t(f_0)$. From the one-parameter semigroup axiom we have:

$$\begin{aligned} f_{t+h} - f_t &= \Phi_{h+t}f_0 - \Phi_t f_0 \\ &= \Phi_h \Phi_t f_0 - \Phi_t f_0 \\ &= (\Phi_h - \Phi_0) f_t. \end{aligned}$$

dividing by h and taking the limit $h \downarrow 0$ in conjunction with strong continuity, we get the time-invariant evolution equation:

$$\frac{df_t}{dt} = \Psi f_t, \text{ where } \Psi := \lim_{h \downarrow 0} \frac{\Phi_h - \Phi_0}{h}. \quad (20)$$

The operator $\Psi : D(\Psi) \rightarrow \mathcal{H}$ is called the generator of the operator family Φ_t and its natural domain $D(\Psi)$ consists of all functions $f \in \mathcal{H}$ for which the above limit makes sense. Typically, this domain will be dense in \mathcal{H} .

Thus, we can interpret Φ_t as the solution operator of an evolution equation. Given that the generator exists, it is possible through various means, for example the spectral theorem [44], to

give meaning to the expression:

$$\Phi_t = e^{t\Psi},$$

which can be used to quickly confirm (at least formally) that:

$$\frac{d\Phi_t}{dt} = \frac{d}{dt}(e^{t\Psi}) = \Psi e^{t\Psi} = \Psi \Phi_t,$$

which corresponds what we already saw in (20).

Remark 3. Given the existence of a generator Ψ , the scaling equivariance axiom can be equivalently written as $\Psi \circ \mathcal{S}_s = \frac{1}{s^\alpha} \mathcal{S}_s \circ \Psi$, revealing that the scaling equivariance can also be understood as a sort of α -homogeneity of the generator.

An easy and illustrative example of a generator together with its operator family is the derivative operator and the family of translation operators in one-dimensional space:

$$(\Phi_t f)(x) = f(x+t), \quad \Psi = \frac{d}{dx}.$$

A well-known related theorem in functional analysis is Stone’s Theorem. This theorem shows that there is a one-to-one correspondence between strongly continuous unitary one-parameter semigroups and (possible unbounded) densely defined self-adjoint operators on a Hilbert space.

In our case getting everything precise is made difficult by the fact that we want to generalize to semifields other than the linear semifield. For example, we can not even directly make sense of (20) for general semifields as there is not necessarily a $-$ operation: we only have \oplus . Given these obstacles, we will not attempt to rigorously prove that every semifield scale-spaces corresponds to a PDE, but will state the related PDEs in our primary cases of interest (Definition 28).

The scaling equivariance says that the scale-space representation of a scaled image should be a scaled version of the scale-space representation of the original image. In a sense we want a scale-space that does not “care” about absolute scale: it should qualitatively looks the same no matter the starting scale of the input. The translation and rotoreflexion equivariance requirements are also not surprising: the Euclidean plane has its natural translation and rotoreflexion symmetries,

and demanding the scale-space to respect these is commonplace.

In the introduction we spend a paragraph explaining that in a PDE-CNN the trainable parameters are the symmetric positive definite matrices $G \in \mathbb{R}^{2 \times 2}$ that determine the inner product that is used on \mathbb{R}^2 , which then changes the look of the corresponding scale-space representation. However, in the axioms above there seems to be no mention of an inner product at first glance. But, in fact, hidden in the roto-reflection equivariance axiom there is the assumption that we use the standard inner product $G = I$.

To see this, we first need to realize that, geometrically, a roto-reflection on the inner product space (\mathbb{R}^2, G) is a matrix Q that satisfies $\langle Qx, Qy \rangle_G = \langle x, y \rangle_G$ for all $x, y \in \mathbb{R}^2$. Taking $G = I$ in this equation results in the requirement that $Q^T Q = I$, i.e. that Q is an orthonormal matrix, just as stated in the roto-reflection equivariance axiom.

The important thing to note is that we can make the assumption $G = I$ in the axioms without loss of generality, and later in Section 6.1 we explain how we bring back the general inner products in the PDE-CNN architecture.

4.2 Examples

Definition 28 (Scale-spaces of Interest).

- a) The Gaussian scale-space over the linear semifield L :

$$(\Phi_t f)(x) = \int_{y \in \mathbb{R}^2} \kappa_t(x, y) \times f(y) \, dy,$$

$$\kappa_t(x, y) = \frac{1}{2\pi t} \exp\left(-\frac{1}{2} \frac{\|x - y\|^2}{t}\right),$$

which correspond to solutions of

$$\frac{\partial f}{\partial t} = \frac{1}{2} \Delta f.$$

The scaling power is $\alpha = 2$.

- b) The (quadratic) root scale-spaces over the root semifields R_p :

$$(\Phi_t f)(x) = \oint_{y \in \mathbb{R}^2}^{R_p} \kappa_t(x, y) \times f(y),$$

$$\kappa_t(x, y) = \frac{1}{\sqrt[p]{2\pi t}} \exp\left(-\frac{1}{2p} \frac{\|x - y\|^2}{t}\right),$$

which correspond to solutions of

$$\frac{\partial f}{\partial t} = \frac{p-1}{f} \frac{1}{2} \|\nabla f\|^2 + \frac{1}{2} \Delta f.$$

The scaling power is $\alpha = 2$.

- c) The (quadratic) logarithmic scale-spaces over the logarithmic semifields L_μ :

$$(\Phi_t f)(x) = \oint_{y \in \mathbb{R}^2}^{L_\mu} \kappa_t(x, y) + f(y),$$

$$\kappa_t(x, y) = -\frac{1}{\mu} \ln(2\pi t) - \frac{1}{2\mu} \frac{\|x - y\|^2}{t},$$

which correspond to solutions of

$$\frac{\partial f}{\partial t} = \mu \frac{1}{2} \|\nabla f\|^2 + \frac{1}{2} \Delta f.$$

The scaling power is $\alpha = 2$.

- d) The α -dilation scale-space over the tropical max semifield T_+ :

$$(\Phi_t f)(x) = \sup_{y \in \mathbb{R}^2} \kappa_t(x, y) + f(y),$$

$$\kappa_t(x, y) = -\frac{t}{\beta} \left(\frac{\|x - y\|}{t} \right)^\beta,$$

with $1/\alpha + 1/\beta = 1$, which correspond to (viscosity) solutions of

$$\frac{\partial f}{\partial t} = \frac{1}{\alpha} \|\nabla f\|^\alpha.$$

The scaling power is α .

- e) The α -erosion scale-space over the tropical min semifield T_- :

$$(\Phi_t f)(x) = \inf_{y \in \mathbb{R}^2} \kappa_t(x, y) + f(y),$$

$$\kappa_t(x, y) = \frac{t}{\beta} \left(\frac{\|x - y\|}{t} \right)^\beta,$$

with $1/\alpha + 1/\beta = 1$, which correspond to (viscosity) solutions of

$$\frac{\partial f}{\partial t} = -\frac{1}{\alpha} \|\nabla f\|^\alpha.$$

The scaling power is α .

The operators Φ_t above solve the corresponding PDEs and one readily checks that the kernels $\kappa_t(\cdot, y)$ satisfy the PDE for all $y \in \mathbb{R}^2$. For example, consider the quadratic ($\alpha = 2$) dilation scale-space and $k_t(x) := \kappa_t(x, 0) = -\frac{1}{2} \frac{\|x\|^2}{t}$:

$$\frac{\partial k_t}{\partial t} = \frac{1}{2} \frac{\|x\|^2}{t^2}, \quad \|\nabla k_t\|^2 = \frac{\|x\|^2}{t^2}.$$

So, indeed, k_t satisfies the dilation PDE. The same check can be done for the other scale-spaces.

Remark 4. The Schrödinger equation also generates a scale-space representation in the space $\mathbb{L}^2(\mathbb{R}^2; \mathbb{C})$, in the sense that it satisfies the linearity axiom and axioms 2-6. However, it does not fit in the theory here as the complex numbers do not form a one-dimensional semifield, and the corresponding kernel $\kappa_t(x, \cdot)$ is not square integrable. In T. Kraakman's thesis [45] PDE-based neural networks using the Schrödinger equation are investigated and implemented. They require more memory than our classical PDE-Based CNNs for only a small performance gain in practice so far.

4.3 Isomorphic Scale-spaces

In Proposition 1 we saw that the nonnegative linear, root, and logarithmic semifields are isomorphic, with the same being true for the tropical ones. It seems natural then that there also exist isomorphisms between the corresponding semifield scale-spaces. Let us start by clarifying what we mean by two semifield scale-spaces being isomorphic.

Definition 29 (Semifield Scale-space Isomorphism). Let R and \tilde{R} be two semifields, and let Φ_t and $\tilde{\Phi}_t$ be two semifield scale-spaces over R and \tilde{R} respectively. We say the two scale-spaces are isomorphic if there exists a semifield isomorphism $\varphi : \tilde{R} \rightarrow R$ such that

$$\Phi_t \circ \mathcal{P}_\varphi = \mathcal{P}_\varphi \circ \tilde{\Phi}_t,$$

where $\mathcal{P}_\varphi : F(\mathbb{R}^2, \tilde{R}) \rightarrow F(\mathbb{R}^2, R)$ is the pointwise operator (9).

Indeed, one can check that in this sense the scale-spaces of interest are isomorphic in the following way, akin to Proposition 1.

Proposition 2 (Scale-Space Isomorphisms).

- The quadratic root scale-spaces over the root semifields R_p are isomorphic to the Gaussian scale-space over the nonnegative linear semifield $L_{\geq 0}$.
- The quadratic logarithmic scale-spaces over the logarithmic semifields L_μ are isomorphic to the Gaussian scale-space over the nonnegative linear semifield $L_{\geq 0}$.
- The α -dilation scale-space over the tropical max semifield T_+ is isomorphic to the α -erosion scale-space over the tropical min semifield T_- .
- Informally, in the limit $\mu \rightarrow \pm\infty$ the quadratic logarithmic scale-spaces over the logarithmic semifields L_μ “converge” to the quadratic ($\alpha = 2$) dilation and erosion scale-spaces of the tropical semifields T_\pm .

Definition 29 also gives us a way to create new (isomorphic) semifield scale-spaces from existing ones in the following way. Take any existing semifield scale-space Φ_t over a semifield R , and let $\varphi : \tilde{R} \rightarrow R$ be any semifield isomorphism. We then simply define the new scale-space $\tilde{\Phi}_t = \mathcal{P}_{\varphi^{-1}} \circ \Phi_t \circ \mathcal{P}_\varphi$ over the semifield \tilde{R} .

In [34] Florack creates nonlinear scale-spaces in exactly this way by performing a pointwise transformation on the Gaussian scale-space and deducing what nonlinear PDE corresponds to the obtained evolution.

More specifically, let $\varphi : R \rightarrow L$ be a monotonic twice continuously differentiable transformation, where $R \subseteq \mathbb{R}$ is some subset of the reals. We start with the isotropic diffusion PDE on \mathbb{R}^2 :

$$\frac{\partial f}{\partial t} = \frac{1}{2} \Delta f.$$

We then define a new evolution $g(x, t) := \varphi^{-1}(f(x, t))$. Let us derive what PDE g obeys. Using the shorthand $\varphi(g) := \mathcal{P}_\varphi(g)$ for a moment, it follows from the equalities:

$$\begin{aligned} \frac{\partial g}{\partial t} &= \frac{\partial}{\partial t} \varphi^{-1}(f) = \frac{1}{\varphi'(g)} \frac{\partial f}{\partial t}, \\ \Delta f &= \Delta(\varphi(g)) = \varphi''(g) \|\nabla g\|^2 + \varphi'(g) \Delta g, \end{aligned}$$

that the PDE that describes the evolution of g is:

$$\frac{\partial g}{\partial t} = \frac{\varphi''(g)}{\varphi'(g)} \frac{1}{2} \|\nabla g\|^2 + \frac{1}{2} \Delta g.$$

Florack suggests setting $\mu := \varphi''/\varphi' = (\ln \varphi')'$ as a constant, as the class of non-trivial (that being non-affine) φ 's is then:

$$\varphi(x) = e^{\mu x} \text{ with } \mu \neq 0, \mu \in \mathbb{R},$$

up to affine transformations. This transformation of the PDE is known as the *Cole-Hopf transformation* [15, p.195]. This is exactly the isomorphism between the logarithmic and linear semifield as seen in Proposition 1, and indeed, with this φ we get the quadratic logarithmic scales spaces:

$$\frac{\partial g}{\partial t} = \mu \frac{1}{2} \|\nabla g\|^2 + \frac{1}{2} \Delta g.$$

In the extreme cases of the transformation, that being $\mu = \pm\infty$, the diffusion part becomes negligible in comparison to the erosion/dilation part, and one can say that the morphological scale-spaces arise.

If we instead choose $\varphi(x) = x^p$ the quadratic root scale-spaces arise:

$$\frac{\partial g}{\partial t} = \frac{p-1}{g} \frac{1}{2} \|\nabla g\|^2 + \frac{1}{2} \Delta g.$$

5 Consequences

In this section we explore the consequences of the semifield scale-spaces axioms (Definition 27). We start by showing that the equivariance axioms of the scale-space representation lead to invariance properties of the kernel $\kappa_t : \mathbb{R}^2 \times \mathbb{R}^2 \rightarrow R$. We then show that, due to the translation equivariance axiom, the semifield scale-space can be written as a semifield convolution with a reduced kernel $k_t : \mathbb{R}^2 \rightarrow R$. From there on out we show Theorem 1 which gives an explicit form of the reduced kernel in the semifield Fourier domain, this being the main theorem of the article.

5.1 Equivariance of Operator becomes Invariance of Kernel

We start by exploring how the translation, roto-reflection, and scaling equivariance axioms on the operator family Φ_t translate to corresponding invariances on the kernel κ_t . The upcoming three lemmas are straightforward, generally known, and basically identical in proof.

Lemma 4 (Translation Invariance). *From the integral operator (axiom 1) and translation equivariance (axiom 5) it follows that the kernel is translation invariant, that is:*

$$\kappa_t(v+x, v+y) = \kappa_t(x, y),$$

for all $x, y, v \in \mathbb{R}^2$ and $t > 0$.

Proof. We rewrite the translation equivariance (axiom 5) as

$$\mathcal{T}_{-v} \circ \Phi_t \circ \mathcal{T}_v = \Phi_t.$$

We apply some dummy function $f \in \mathcal{H}$ and evaluate it at some dummy position $x \in \mathbb{R}^2$:

$$((\mathcal{T}_{-v} \circ \Phi_t \circ \mathcal{T}_v)(f))(x) = (\Phi_t(f))(x).$$

Using the definition of the translation operator \mathcal{T}_v (6) and the integral operator axiom we expand this into:

$$\oint_{y \in \mathbb{R}^2} \kappa_t(v+x, y) \otimes f(-v+y) = \oint_{y \in \mathbb{R}^2} \kappa_t(x, y) \otimes f(y).$$

Using the translation invariance property (12) of the semifield integration gives:

$$\oint_{y \in \mathbb{R}^2} \kappa_t(v+x, v+y) \otimes f(y) = \oint_{y \in \mathbb{R}^2} \kappa_t(x, y) \otimes f(y).$$

Given that this should hold for all $f \in \mathcal{H}$ we can conclude:

$$\kappa_t(v+x, v+y) = \kappa_t(x, y).$$

□

Lemma 5 (Rotoreflexion Invariance). *From the integral operator (axiom 1) and the roto-reflection equivariance (axiom 6) it follows that the kernel is roto-reflection invariant, that is:*

$$\kappa_t(Qx, Qy) = \kappa_t(x, y),$$

for all orthonormal $Q \in \mathbb{R}^{2 \times 2}$, $x, y \in \mathbb{R}^2$, and $t > 0$.

Proof. We rewrite the roto-reflection equivariance (axiom 6) as

$$\mathcal{R}_{Q^{-1}} \circ \Phi_t \circ \mathcal{R}_Q = \Phi_t.$$

We apply some dummy function $f \in \mathcal{H}$ and evaluate it at some dummy position $x \in \mathbb{R}^2$:

$$((\mathcal{R}_{Q^{-1}} \circ \Phi_t \circ \mathcal{R}_Q)(f))(x) = (\Phi_t(f))(x).$$

Using the definition of the rotoreflection operator \mathcal{R}_Q (7) and integral operator axiom we expand this to:

$$\oint_{y \in \mathbb{R}^2} \kappa_t(Qx, -y) \otimes f(Q^{-1}y) = \oint_{y \in \mathbb{R}^2} \kappa_t(x, y) \otimes f(y).$$

Using the rotoreflection invariance property (13) of the semifield integration gives:

$$\oint_{y \in \mathbb{R}^2} \kappa_t(Qx, Qy) \otimes f(y) = \oint_{y \in \mathbb{R}^2} \kappa_t(x, y) \otimes f(y).$$

Given that this should hold for all $f \in \mathcal{H}$ we can conclude:

$$\kappa_t(Qx, Qy) = \kappa_t(x, y).$$

□

Lemma 6 (Scale Invariance). *From the integral operator (axiom 1) and scaling equivariance (axiom 4) it follows that the kernel is scale invariant, that is:*

$$\chi(s) \otimes \kappa_{s^{\alpha_t}}(sx, sy) = \kappa_t(x, y).$$

for all $x, y \in \mathbb{R}^2$ and $s, t > 0$.

Proof. We rewrite the scaling equivariance (axiom 4) as

$$\mathcal{S}_{1/s} \circ \Phi_{s^{\alpha_t}} \circ \mathcal{S}_s = \Phi_t.$$

We apply some dummy function $f \in \mathcal{H}$ and evaluate it at some dummy position $x \in \mathbb{R}^2$:

$$((\mathcal{S}_{1/s} \circ \Phi_{s^{\alpha_t}} \circ \mathcal{S}_s)(f))(x) = (\Phi_t(f))(x).$$

Using the definition of the scaling operator \mathcal{S}_s (8) and integral operator axiom we expand this to:

$$\oint_{y \in \mathbb{R}^2} \kappa_{s^{\alpha_t}}(sx, y) \otimes f(y/s) = \oint_{y \in \mathbb{R}^2} \kappa_t(x, y) \otimes f(y).$$

Using the scaling property (14) of the semifield integration gives:

$$\chi(s) \otimes \oint_y \kappa_{s^{\alpha_t}}(sx, sy) \otimes f(y) = \oint_y \kappa_t(x, y) \otimes f(y).$$

Given that this should hold for all $f \in \mathcal{H}$ we conclude:

$$\chi(s) \otimes \kappa_{s^{\alpha_t}}(sx, sy) = \kappa_t(x, y).$$

□

Consider now Lemma 4. Because we can freely choose the translation v , we can also choose $v = -y$:

$$\kappa_t(x, y) = \kappa_t(x - y, 0) =: k_t(x - y).$$

We thus see that κ_t is completely characterized by its behaviour on $\kappa_t(\cdot, 0)$, which we define as the reduced kernel $k_t : \mathbb{R}^2 \rightarrow R$. Plugging this new-found knowledge back into the integral operator axiom we get the following result.

Lemma 7 (Translation Equivariance implies Semifield Convolution). *Consider the integral operator (axiom 1) and translation equivariance (axiom 5). Define the reduced kernel $k_t(x) = \kappa_t(x, 0)$. We can write the scale-space operator Φ_t as a semifield convolution:*

$$\Phi_t f = k_t \circledast f.$$

Proof. This follows immediately from Lemma 4.

$$\begin{aligned} (\Phi_t f)(x) &= \oint_{y \in \mathbb{R}^2} \kappa_t(x, y) \otimes f(y) \\ &= \oint_{y \in \mathbb{R}^2} \kappa_t(x - y, 0) \otimes f(y) \\ &= \oint_{y \in \mathbb{R}^2} k_t(-y + x) \otimes f(y) \\ &= (k_t \circledast f)(x). \end{aligned}$$

□

Lemma 8 (Convolution Property of Reduced Kernel). *From the integral operator (axiom 1), the one-parameter semigroup (axiom 2), the strong continuity (axiom 3), and the translation equivariance (axiom 5), it follows that the reduced kernel $k_t(x) = \kappa_t(x, 0)$ satisfies:*

$$k_s \circledast k_t = k_{s+t} \text{ for all } t, s > 0.$$

Proof. We have already seen in Lemma 7 that the integral operator axiom and the translation

equivariance axiom imply that

$$\Phi_t f = k_t \circledast f.$$

If we use this formula together with the one-parameter semigroup property axiom we get

$$k_s \circledast (k_t \circledast f) = k_{s+t} \circledast f.$$

Using associativity of semifield convolution (16) on the l.h.s.:

$$(k_s \circledast k_t) \circledast f = k_{s+t} \circledast f.$$

We are free to choose $f = k_\varepsilon$ for $\varepsilon > 0$:

$$(k_s \circledast k_t) \circledast k_\varepsilon = k_{s+t} \circledast k_\varepsilon.$$

From the strong continuity axiom we know that $\lim_{\varepsilon \rightarrow 0} k_\varepsilon \circledast k_t = k_t$, thus, after taking this limit, we can conclude:

$$k_s \circledast k_t = k_{s+t}.$$

□

5.2 Towards the Semifield Fourier Domain

We see that to move forward we need a way to efficiently work with semifield convolutions. The semifield Fourier transform (Definition 25) has the important property of turning convolutions into much more wieldy pointwise multiplication. This is why we translate all previous lemmas to the semifield Fourier domain using the semifield Fourier transform.

Lemma 9. *Consider all axioms of a semifield scale-space (Definition 27). The reduced kernel $k_t(x) := \kappa_t(\cdot, 0)$ in the semifield Fourier domain $\hat{k}_t = \mathcal{F}_R(k_t)$ satisfies*

$$\hat{k}_t(Q\omega) = \hat{k}_t(\omega), \quad (21)$$

$$\hat{k}_{s\alpha_t}(\omega/s) = \hat{k}_t(\omega), \quad (22)$$

$$\hat{k}_s(\omega) \otimes \hat{k}_t(\omega) = \hat{k}_{s+t}(\omega), \quad (23)$$

for all orthonormal $Q \in \mathbb{R}^{2 \times 2}$, $\omega \in \mathbb{R}^2$, and $s, t > 0$.

Proof. Lemma 5 tells us that

$$\kappa_t(Qx, Qy) = \kappa_t(x, y).$$

Translating this to the reduced kernel k_t gives

$$k_t(Qx) = k_t(x).$$

Taking the semifield Fourier transform on both sides, and using the rotoreflection equivariance property of the Fourier transform (18), we get:

$$\hat{k}_t(Q\omega) = \hat{k}_t(\omega).$$

Lemma 6 also tells us that

$$\chi(s) \otimes \kappa_{s\alpha_t}(sx, sy) = \kappa_t(x, y).$$

Translating this to the reduced kernel k_t gives

$$\chi(s) \otimes k_{s\alpha_t}(sx) = k_t(x).$$

Taking the semifield Fourier transform on both sides, and using the scaling equivariance property of the Fourier transform (19), we get:

$$\chi(s) \otimes \chi(1/s) \otimes \hat{k}_{s\alpha_t}(\omega/s) = \hat{k}_t(\omega).$$

Using that χ is a homomorphism we know that $\chi(s) \otimes \chi(1/s) = \chi(s/s) = \chi(1) = \mathbb{1}$, so we can simplify this to

$$\hat{k}_{s\alpha_t}(\omega/s) = \hat{k}_t(\omega).$$

Lemma 8 tells us that

$$k_s \circledast k_t = k_{s+t}.$$

Taking the semifield Fourier transform on both sides, and using the convolution property of the Fourier transform (17), we get:

$$\hat{k}_s \otimes \hat{k}_t = \hat{k}_{s+t}.$$

□

Let us check if the reduced kernels of the scale-spaces of interest indeed satisfy the properties listed in the previous lemma by inspecting their Fourier transforms.

Proposition 3 (Semifield Fourier Transform of Kernels of Interest). *Consider the employed semifield Fourier transforms (Definition 26) and the semifield scale-spaces of interest (Definition 28). Let $k_t(x) := \kappa_t(\cdot, 0)$ be the reduced kernel and $\hat{k}_t = \mathcal{F}_R(k_t)$ its semifield Fourier transform.*

- a) *For the Gaussian scale-space over the linear semifield L we have:*

$$\hat{k}_t^L(\omega) = \exp\left(-\frac{1}{2}t\|\omega\|^2\right).$$

- b) *For the quadratic root scale-spaces over the root semifields R_p we have:*

$$\hat{k}_t^{R_p}(\omega) = \exp\left(-\frac{1}{2p}t\|\omega\|^2\right).$$

- c) *For the quadratic logarithmic scale-spaces over the logarithm semifields L_μ we have:*

$$\hat{k}_t^{L_\mu}(\omega) = -\frac{1}{2\mu}t\|\omega\|^2.$$

- d) *For the α -dilation scale-space over the tropical max semifield T_+ we have:*

$$\hat{k}_t^{T_+}(\omega) = \frac{1}{\alpha}t\|\omega\|^\alpha.$$

- e) *For the α -erosion scale-space over the tropical min semifield T_- we have:*

$$\hat{k}_t^{T_-}(\omega) = -\frac{1}{\alpha}t\|\omega\|^\alpha.$$

5.3 Explicit Form of the Reduced Kernel

With the results derived above we are now ready to derive the explicit form of the reduced kernel in the Fourier domain \hat{k}_t , and, in turn, an expression for the reduced kernel k_t . But to succinctly state this explicit form we need one extra ingredient: semifield exponentiation, i.e. a generalization of repeated semifield multiplication.

Definition 30 (Semifield Exponentiation). Let $R = (R, 0, 1, \oplus, \otimes)$ be a one-dimensional metric semifield. The semifield exponentiation \exp_R :

$\mathbb{R} \rightarrow R$ is defined as the (up to time scaling unique⁷) mapping that satisfies⁸:

$$\begin{aligned} \exp_R(s) \otimes \exp_R(t) &= \exp_R(s+t) \text{ for all } s, t \in \mathbb{R}, \\ \exp_R(0) &= 1, \\ \lim_{t \rightarrow \infty} \exp_R(t) &= 0. \end{aligned}$$

To distinguish the semifield exponentiation from regular exponentiation we always indicate the former with the semifield in the subscript, and the latter without any subscript.

Definition 31 (Employed Semifield Exponentiation).

- a) In the (nonnegative) linear semifield L case we have $\exp_L(t) = \exp(-t)$.
- b) In the root semifields R_p case we have $\exp_{R_p}(t) = \exp(-t)$.
- c) In the logarithmic semifields L_μ case we have $\exp_{L_\mu}(t) = -\text{sign}(\mu)t$.
- d) In the tropical max semifield T_+ case we have $\exp_{T_+}(t) = -t$.
- e) In the tropical min semifield T_- case we have $\exp_{T_-}(t) = t$.

Theorem 1 (Explicit form Reduced Kernel). *Let R be a one-dimensional metric semifield, \mathcal{F}_R the semifield Fourier transform (Definition 25), and \exp_R the semifield exponentiation (Definition 30). Consider all axioms of a semifield scale-space (Definition 27). We have that the reduced kernel k_t is (up to a time scaling) equal to:*

$$\begin{aligned} \hat{k}_t(\omega) &= \exp_R(\|\omega\|^\alpha t), \\ k_t(x) &= (\mathcal{F}_R^{-1} \hat{k}_t)(x), \end{aligned}$$

where α is the scaling power (axiom 4).

Before we continue with the proof, we can check that, indeed, all semifield Fourier transforms of the reduced kernels, as listed in Proposition 3, have this stated form.

Proof. Consider the reduced kernel \hat{k}_t in the Fourier domain and all its properties as listed in

⁷The connected part of (R, \otimes) that contains 1 is a one-dimensional Lie group. Semifield exponentiation is the Lie group exponential and is determined by a one-dimensional tangent vector at the identity, thus giving us the up to scaling uniqueness.

⁸The requirement $\exp_R(0) = 1$ doesn't need to be included, it follows from the one-parameter semigroup property by plugging in $t = 0$, together with the existence of multiplicative inverses.

Lemma 9. Due to the rotoreflectional symmetry (21) we will abuse notation slightly and write

$$\hat{k}_t(\omega) = \hat{k}_t(\|\omega\|) = \hat{k}_t(r),$$

where $r = \|\omega\|$. Taking $s = r > 0$ in the scaling invariance (22) we get

$$\hat{k}_t(r) = \hat{k}_{r\alpha_t}(1) \text{ for } r > 0.$$

Due to the one-parameter semigroup property (23) and $t \mapsto \hat{k}_t(\omega)$ being continuous, we have (up to a time scaling)

$$\hat{k}_t(1) = \exp_R(t) \text{ or } \hat{k}_t(1) = 0.$$

We are not interested in the $\hat{k}_t(1) = 0$ case as it would imply, together with the previous equation, that \hat{k}_t is identically zero, corresponding to a non-relevant scale-space. Combining the equations found so far we get

$$\hat{k}_t(r) = \exp_R(r^\alpha t) \text{ for } r > 0.$$

which we can extend to $r = 0$ by continuity. Taking the inverse semifield Fourier transform concludes the proof. \square

The up-to-a-time-scaling non-uniqueness is something we can *not* avoid as every semifield scale-space Φ_t corresponds to an infinite family of scale-spaces $\hat{\Phi}_t = \Phi_{st}$ for every $s > 0$.

The above theorem shows that every (one dimensional metric) semifield R corresponds to a unique one-parameter family of semifield scale-spaces, where the scaling power α acts as the parameter.

There is one caveat here though, and that is that not every α necessarily results in a \tilde{k}_t which is in the domain of the used inverse semifield Fourier transform. For example, in the tropical semifields the case $\alpha = 1$ results in a \tilde{k}_t which we cannot insert into the inverse transforms listed in Definition 26.

6 Experiments

6.1 Architecture

Consider any one-dimensional metric semifield R and a corresponding semifield scale-space Φ_t . As

Lemma 7 shows, we can write the scale-space $\Phi_t f$ of a (appropriate) function $f : \mathbb{R}^2 \rightarrow R$ as $\Phi_t f = k_t \circledast f$ where $k_t : \mathbb{R}^2 \rightarrow R$ is the reduced kernel, and \circledast is the semifield convolution. We want to implement these semifield scale-spaces to use them within the design of our PDE-CNNs. However, in practice, we can not work with general signals defined on the continuum of \mathbb{R}^2 , and we need to discretize our setting.

As is usual in machine learning we imagine images $f : \mathbb{R}^2 \rightarrow R$ as sampled images $\tilde{f} : Z \rightarrow R$ on a grid $Z \subset \mathbb{R}^2$ such that $\tilde{f}(z) = f(z)$ for all grid points $z \in Z$. We idealize the grid as the infinite integer grid \mathbb{Z}^2 here for the sake of simplicity (we have no boundary concerns). Let $\tilde{f}, \tilde{k} : \mathbb{Z}^2 \rightarrow R$ be the discretized versions of an image f and any kernel k . The discrete semifield convolution \circledast^9 is defined as

$$(\tilde{k} \circledast \tilde{f})[i, j] = \bigoplus_{m, n \in \mathbb{Z}^2} \tilde{k}[-m + i, -n + j] \circledast \tilde{f}[m, n],$$

where we have used the notation $[\cdot, \cdot]$ to emphasize the discrete nature.

With the discrete semifield convolution we can write down the formula for a PDE sublayer in the PDE-CNN. The input of a PDE sublayer consists of signals $\tilde{f}_i : \mathbb{Z}^2 \rightarrow R$ and matrices $H_i \in \mathbb{R}^{2 \times 2}$ with $i = 1, \dots, C$, and C being the amount of channels. The matrices H_i act as the learnable parameters of the layer. We consider the continuous scale-space kernel $k_t : \mathbb{R}^2 \rightarrow R$ and create the discretized kernels $\tilde{k}_i : \mathbb{Z}^2 \rightarrow R$ by defining $\tilde{k}_i(x) = k_1(H_i x)^{10}$. We then perform the discrete semifield convolutions to acquire our outputs $\tilde{g}_i : \mathbb{Z}^2 \rightarrow R^{11}$:

$$\begin{aligned} &\text{PDE sublayer:} \\ &\tilde{g}_i = \tilde{k}_i \circledast \tilde{f}_i. \end{aligned} \tag{24}$$

The matrices H_i require some explanation. As already touched upon in Section 4.1, in the semifield scale-space axioms we implicitly assumed the standard inner product $\langle x, y \rangle = x^T y$ on \mathbb{R}^2 , but this is not the only one we can choose. By choosing

⁹We overload the semifield convolution symbol \circledast here.

¹⁰Without loss of generality, we may take $t = 1$ in our scale-space kernel k_t as a scaling in t can be captured in H .

¹¹Every kernel is only convolved with a single input image, this is also known as a depthwise convolution.

the inner product to be

$$\langle x, y \rangle = x^T G y, \quad G = H^T H$$

for any matrix H^{12} we get a scale-space representation that is complete identical, albeit “stretched” with respect to the coordinates. By considering kernels of the form $k_t(Hx)$ we effectively include the possibility of processing the image with a different inner product¹³.

At this point some clarification of the terminology might be in order. The PDE sublayer, as described in the formula above, seems to have nothing to do with a PDE at first glance. However, remember that every semifield scale-space Φ_t over a semifield R can be associated with a PDE, and the PDE sublayer is effectively a solver for the corresponding initial value problem. The examples in Definition 28 clarify this.

Alongside the PDE sublayers that correspond to semifield scale-spaces we also have the convection PDE sublayer. The convection sublayer effectively solves the convection PDE by translating images. The input of a convection PDE sublayer consists of images $\tilde{f}_i : \mathbb{Z}^2 \rightarrow R$ and vectors $v_i \in \mathbb{R}^2$ with $i = 1, \dots, C$, and C being the amount of channels. The vectors v_i act as the learnable parameters of the layer. The output signals $\tilde{g}_i : \mathbb{Z}^2 \rightarrow R$ are obtained through bilinear interpolating (Interp) the inputs at the appropriate positions:

Convection sublayer:

$$\tilde{g}_i[m, n] = \text{Interp}(\tilde{f}_i, m - (v_i)_1, n - (v_i)_2). \quad (25)$$

The final ingredient we need is the affine layer¹⁴ which is defined as follows. The input consists of channels $\tilde{f}_i : \mathbb{Z}^2 \rightarrow \mathbb{R}$, weights $w_{ij} \in \mathbb{R}$, and biases $b_j \in \mathbb{R}$, with $i = 1, \dots, C_i$, $j = 1, \dots, C_o$, and C_i, C_o being the amount of input and output channels respectively. The weights w_{ij} and biases b_j act as the learnable parameters of the layer. We then perform the following pointwise computation

¹²The matrix $G = H^T H$ is by construction symmetric positive definite (SPD) as required, and relieves us from coding a SPD constraint.

¹³We can compare this to the PDE-G-CNN architecture which effectively learns left-invariant metric tensor fields on $\text{SE}(2)$.

¹⁴Also known as a 1x1 convolutional layer with bias

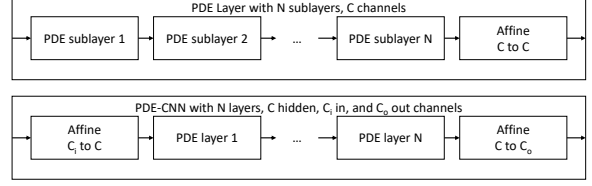


Fig. 7: The architecture of a N -layer PDE-CNN with C channels. A PDE sublayer is either of the form (24) or (25).

to get the C_o outputs $\tilde{g}_j : \mathbb{Z}^2 \rightarrow R$

Affine layer:

$$\tilde{g}_j = b_j + \sum_{i=1}^{C_i} w_{ij} \tilde{f}_i.$$

By concatenating various PDE sublayers, that being either a sublayer that corresponds to a scale-space or a convection sublayer, with an affine combination layer at the end we form a PDE layer. Multiple PDE layers after each other with an affine layer at the start and end creates a PDE-CNN. The architecture is illustrated in Figure 7.

6.2 Data Efficiency of PDE-CNNs on DRIVE dataset

The data efficiency of PDE-G-CNNs is already verified in [4], but whether this desirable property this holds in the PDE-CNN case is still left untested. Our first experiment is therefore testing the data efficiency of a PDE-CNN. The PDE-CNN we consider here employs three PDEs within its PDE layers: convection, α -dilation, and α -erosion, just as in the papers [1, 4–6].

We will be testing on the DRIVE dataset [3], which consists of 584×565 8bit RGB color fundus images, with the goal being vessel segmentation. In Figure 8 one can see an example of such an image and its segmentation. The dataset consist of a training set of 20 images, and a test set of 20 images. All images are rescaled within the $[0, 1]$ range by dividing by 255. We divided the training set into 2880 overlapping patches of 64×64 . Patches that contain no annotation, i.e. patches that are essentially completely within the black mask, are removed, leaving us with 2409 patches.

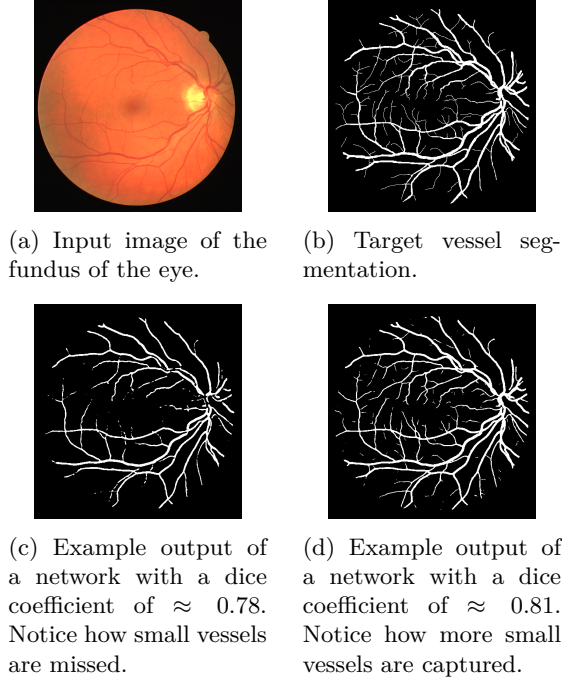


Fig. 8: One instance of an input and its corresponding target segmentation from the DRIVE dataset, together with two example outputs of networks with different dice coefficients.

As a baseline we consider a 6-layer CNN with 25 662 parameters from [4], and compare this against a 6-layer 24-channel PDE-CNN with 5 280 parameters. These networks have been designed to give a satisfactory Dice coefficient of $\gtrapprox 0.80$ on the test set when trained on the complete training set.

Following the method in [4], we randomly take 1% to 100% of the training data. We train on batches consisting of 8 patches. We empirically found that a higher batch size results in a worse test set accuracy. We use the AdamW optimizer with an initial learning rate of 0.01 that decays linearly to 0.001 over the first 1 000 batches. The beta, epsilon and weight decay parameters of AdamW are kept at their default values of (0.9, 0.999), 10^{-8} , and 0.01. During training we keep track of the Dice coefficient on the test set and the best one is stored. We train until this performance on the test set no longer increases, which happens within 15 000 batches. We repeat this 5 times for every possible situation to obtain an average performance.

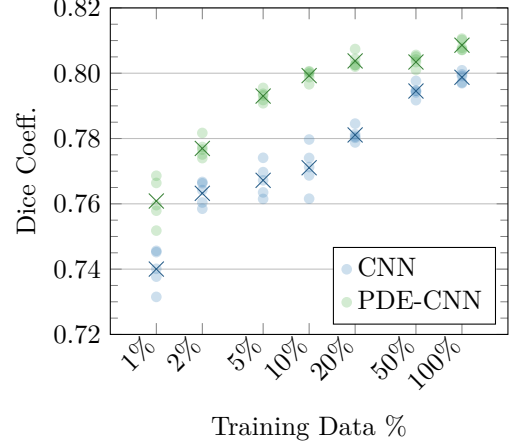


Fig. 9: A scatterplot of the performance of a 6-layer CNN (25 662 parameters) and PDE-CNN (5 280 parameters) on the DRIVE dataset, when trained multiple times on varying amounts of training data. The crosses indicate the mean.

The result can be found in Figure 9. We see that on the DRIVE dataset, in comparison with a standard CNN, the PDE-CNN not only features fewer parameters but also showcases competitive performance and increased data efficiency. This mirrors the results found in [4], but this time for a PDE-CNN instead of the $G = \text{SE}(2)$ PDE-G-CNN considered there.

6.3 Other Semifields within PDE-CNNs

The second experiment examines how including the discussed semifields affects performance. This means we add PDE sublayers corresponding to the scale-spaces (Definition 27) that arise naturally from the semifields, as shown in Theorem 1. To keep focus we only consider semifields we have already discussed, that being the linear L , tropical min T_- , tropical max T_+ , root R_p , and logarithmic L_μ semifields. In concrete terms, this means we implement the scale-spaces listed in Definition 28.

The networks that we consider always include the convection PDE sublayer at the start of the PDE layer. The PDE-CNNs will always consist of 6 PDE layers, 32 channels, and have parameter count of approximately 9 500 on average, which changes with the amount of semifields we add.

Our methodology is identical to Section 6.2, however this time we always train on the complete DRIVE dataset. This allows us to compare the results found in this section with the ones in Figure 9. We found that training is a bit slower with the logarithmic and root semifields, so we increased the training to 20 000 batches.

We empirically found that adding the linear semifield, that is we add a PDE sublayer corresponding to the Gaussian scale-space, does *not* affect the performance of any the networks. This can be explained by noticing that such a PDE sublayer can be emulated completely and effectively by the convection sublayer together with the affine combination sublayer, which are always components of the PDE-CNNs we consider here. For this reason we have omitted the linear semifield PDE sublayers altogether. This is in agreement with the results found in [46, p.28].

The result can be found in Figure 10. We observe multiple things:

- Adding semifields to the existing PDE-CNN architecture, which only employ the tropical semifields and convection, may enhance performance, albeit not significantly, as observed in the case of $\{T_+, T_-, L_\mu\}$.
- The inclusion of the tropical min semifield T_- *always* increases performance, most starkly seen when going from $\{L_\mu\}$ to $\{T_-, L_\mu\}$.
- Adding semifields does *not* necessarily improve performance, as is evident from the last row when compared to the two-semifield models in the middle rows.
- The inclusion of the root semifield R_p seems to make the training less stable, as indicated by the increase in spread within the scatter plot at the respective rows.

It is worth mentioning however that these results might be specific to the DRIVE dataset.

7 Conclusion

PDE-CNNs are an interesting alternative to CNNs in the sense that their constituents, this being solvers of PDEs that generate scale-spaces, are geometrically meaningful and interpretable.

The existing PDE-CNN framework utilizes four PDEs: convection, diffusion, dilation, and erosion. Through the introduction of semifield scale-spaces (Definition 27) we demonstrate the

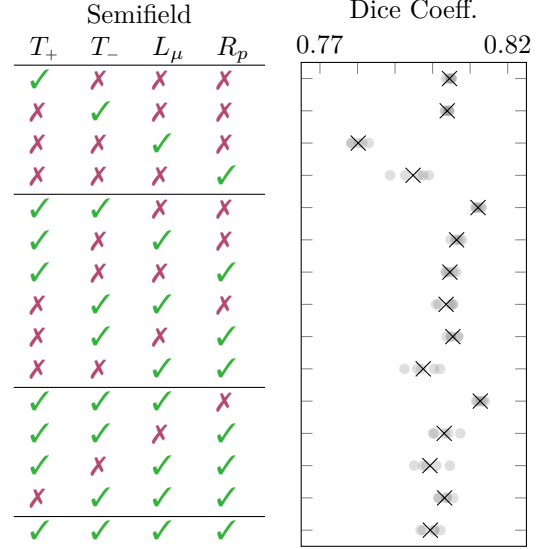


Fig. 10: A scatterplot of the performance of a 6-layer PDE-CNN on the DRIVE dataset, with various designs of the PDE layer as indicated in the table on the left. The crosses indicate the mean. The rows are organized according to the amount of semifields included in the model.

presence of a broad class of PDEs that remain unutilized within the PDE-CNN paradigm.

The theory of semifields scale-spaces is expressive and encapsulates a large class of known scale-spaces. Theorem 1 shows that every semifield gives rise to a one-parameter family of semifield scale-spaces. This indicates that the generalization to semifields is one that is not too general and definitely fruitful.

In Section 6.2 we empirically verified that on the DRIVE dataset that PDE-CNNs, just like PDE-G-CNNs, when compared to traditional CNNs, require less training data, have fewer parameters, and increased performance.

In Section 6.3 we experimented on the inclusion of various semifields and their corresponding scale-spaces within PDE layers of a PDE-CNN. We see that the thought “more semifields means better performance” is incorrect, and that it is not clear if the addition of more semifields into the already existing PDE-CNN framework is worth the effort. However, in all cases inclusion of the tropical semifield improved the result, advocating for tropical algebras in PDE-based neural networks.

Further Research

When comparing the results of PDE-CNNs on the DRIVE dataset here to the $G = \text{SE}(2)$ PDE-G-CNNs results in [4], the accuracy is essentially the same (Dice ≈ 0.81), but there is a trade-off between memory usage and parameter reduction.

The $\text{SE}(2)$ variant has less parameters (2560) but, due to the feature maps being scalar fields on $\text{SE}(2)$, uses more memory, that being $O \times H \times W$ scalars per feature map. Here O refers to the amount of orientations (typically 8), H to the height of the images, and W to the width.

Conversely, the \mathbb{R}^2 variant has more parameters (5280) but uses much less memory; $H \times W$ scalars per feature map. This means that in some applications the PDE-CNN architecture might be preferable. However, the goal of the work here was not to compare PDE-CNNs to PDE-G-CNNs and the observations here only apply to the DRIVE dataset. Further research is needed to properly compare both architectures.

Declarations

Acknowledgements

We thank Adrien Castella [46] for the initial Python implementation of the \mathbb{R}^2 convection, diffusion, dilation and erosion PDE sublayers <https://github.com/adrien-castella/PDE-based-CNNs>.

Funding

We gratefully acknowledge the Dutch Foundation of Science NWO for funding of VICI 2020 Exact Sciences (Duits, Geometric learning for Image Analysis, VI.C.202-031 <https://www.nwo.nl/en/projects/vic202031>).

Availability of Data and Code

The DRIVE dataset [3] can (currently¹⁵) be found at <https://drive.grand-challenge.org/>. The LieTorch package is public and can be found at <https://gitlab.com/bsmetsjr/lietorch>. The original PDE-CNN implementation can be found at <https://github.com/adrien-castella/PDE-based-CNNs>.

¹⁵The old address was <https://web.archive.org/web/20191003101812/http://www.isi.uu.nl/Research/Databases/DRIVE/>.

Appendix A Semifield Fourier Transforms

Lemma 10. *The employed semifield Fourier transforms indeed satisfy Definition 25.*

Proof. In the linear semifield L case we know that the familiar Fourier transform satisfies the definition.

As for the root and logarithmic semifields, being isomorphic to the linear semifield, we can quickly deduce that they also satisfy the definitions through the equalities

$$\begin{aligned}\mathcal{F}_{L_\mu} &= \mathcal{P}_{\varphi_\mu^{-1}} \circ \mathcal{F}_L \circ \mathcal{P}_{\varphi_\mu}, \\ \mathcal{F}_{R_p} &= \mathcal{P}_{\varphi_p^{-1}} \circ \mathcal{F}_L \circ \mathcal{P}_{\varphi_p},\end{aligned}$$

where \mathcal{P} is the pointwise operator (9), $\varphi_\mu(x) = e^{\mu x}$ the semifield isomorphism $\varphi_\mu : L_\mu \rightarrow L_{\geq 0}$, and $\varphi_p(x) = x^p$ the semifield isomorphism $\varphi_p : R_p \rightarrow L_{\geq 0}$. For example, to show that \mathcal{F}_{L_μ} satisfies the convolution property:

$$\begin{aligned}\mathcal{F}_{L_\mu}(f \otimes g) &= \mathcal{P}_{\varphi_\mu^{-1}} \mathcal{F}_L \mathcal{P}_{\varphi_\mu}(f \otimes g) \\ &= \mathcal{P}_{\varphi_\mu^{-1}} \mathcal{F}_L((\mathcal{P}_{\varphi_\mu} f) * (\mathcal{P}_{\varphi_\mu} g)) \\ &= \mathcal{P}_{\varphi_\mu^{-1}}((\mathcal{F}_L \mathcal{P}_{\varphi_\mu} f) \times (\mathcal{F}_L \mathcal{P}_{\varphi_\mu} g)) \\ &= (\mathcal{P}_{\varphi_\mu^{-1}} \mathcal{F}_L \mathcal{P}_{\varphi_\mu} f) \otimes (\mathcal{P}_{\varphi_\mu^{-1}} \mathcal{F}_L \mathcal{P}_{\varphi_\mu} g) \\ &= (\mathcal{F}_{L_\mu} f) \otimes (\mathcal{F}_{L_\mu} g),\end{aligned}$$

where \otimes and \times are the semifield convolution and multiplication of L_μ and where \times denotes the standard pointwise product of functions. In the above derivation we have used that

$$\begin{aligned}\mathcal{P}_{\varphi_\mu}(f \otimes g) &= (\mathcal{P}_{\varphi_\mu} f) * (\mathcal{P}_{\varphi_\mu} g), \\ \mathcal{P}_{\varphi_\mu^{-1}}(f \times g) &= (\mathcal{P}_{\varphi_\mu^{-1}} f) \otimes (\mathcal{P}_{\varphi_\mu^{-1}} g),\end{aligned}$$

and that \mathcal{F}_L has the convolution property.

Consider now the tropical max semifield T_+ . That \mathcal{F}_{T_+} satisfies the linearity, equivariences, and the zero-frequency properties is immediate. As for

the convolution property we have

$$\begin{aligned}
& (\mathcal{F}_{T_+}(f \otimes g))(\omega) \\
&= \sup_x (f \otimes g)(x) - \omega \cdot x \\
&= \sup_x (\sup_y f(x-y) + g(y)) - \omega \cdot x \\
&= \sup_x (\sup_{x_1+x_2=x} f(x_1) + g(x_2)) - \omega \cdot x \\
&= \sup_{x_1, x_2} f(x_1) + g(x_2) - \omega \cdot (x_1 + x_2) \\
&= (\sup_{x_1} f(x_1) - \omega \cdot x_1) + (\sup_{x_2} g(x_2) - \omega \cdot x_2) \\
&= (\mathcal{F}_{T_+}f)(\omega) \otimes (\mathcal{F}_{T_+}g)(\omega),
\end{aligned}$$

where \otimes and \otimes are the tropical max T_+ multiplication and convolution. For the invertibility we refer to the Fenchel biconjugation theorem [47, Thm.4.2.1]. That the tropical min semifield Fourier transform \mathcal{F}_{T_-} satisfies all properties follows from the fact that T_- is semifield isomorphic to T_+ with the isomorphism being $\phi(x) = -x$. \square

Appendix B Tropical Integration

Proposition 4. *The natural integration of sum-approachable and bounded from above functions $f : \mathbb{R}^2 \rightarrow T_+$ is*

$$\oint^{T_+} f = \sup_{x \in \mathbb{R}^2} f(x).$$

The natural integration of sum-approachable and bounded from below functions $f : \mathbb{R}^2 \rightarrow T_-$ is

$$\oint^{T_-} f = \inf_{x \in \mathbb{R}^2} f(x).$$

Proof. We will only prove this for the tropical max semifield T_+ , the tropical min semifield case goes completely analogously. As we are working with T_+ we remind ourselves that we have $\oplus = \max$, $\otimes = +$, $\mu_{T_+}(A) = 0$, and

$$\mathbb{1}_A(x) = \begin{cases} 0 & \text{if } x \in A \\ -\infty & \text{otherwise} \end{cases}.$$

The function f , being sum-approachable and bounded from above, is pointwise defined by the

limit

$$f(x) = \lim_{n \rightarrow \infty} \bigoplus_{i=1}^n a_i \otimes \mathbb{1}_{A_i}(x),$$

with A_i non-empty and a_i bounded from above. We define its natural integral by

$$\begin{aligned}
\oint f &:= \lim_{n \rightarrow \infty} \oint \left(\bigoplus_{i=1}^n a_i \otimes \mathbb{1}_{A_i} \right) \\
&= \lim_{n \rightarrow \infty} \bigoplus_{i=1}^n a_i \otimes \mu(A) \\
&= \lim_{n \rightarrow \infty} \max_{i=1, \dots, n} a_i + 0 \\
&= \sup_{i \in \mathbb{N}} a_i,
\end{aligned}$$

where the second equality is by the linearity of the integration (10) and the indicator function property (11).

Similarly, we have

$$\begin{aligned}
\sup_{x \in \mathbb{R}^2} f(x) &= \sup_{x \in \mathbb{R}^2} \lim_{n \rightarrow \infty} \bigoplus_{i=1}^n a_i \otimes \mathbb{1}_{A_i}(x) \\
&= \sup_{x \in \mathbb{R}^2} \lim_{n \rightarrow \infty} \max_{i=1, \dots, n} a_i + \mathbb{1}_{A_i}(x) \\
&= \sup_{x \in \mathbb{R}^2} \sup_{i \in \mathbb{N}} a_i + \mathbb{1}_{A_i}(x) \\
&= \sup_{i \in \mathbb{N}} \sup_{x \in \mathbb{R}^2} a_i + \mathbb{1}_{A_i}(x) \\
&= \sup_{i \in \mathbb{N}} a_i,
\end{aligned}$$

where in the fourth equality we interchanged the order of suprema, and in the fifth equality we used the definition of $\mathbb{1}_{A_i}$.

Combining these two results, it follows that

$$\oint f = \sup_{x \in \mathbb{R}^2} f(x)$$

is the natural tropical max semifield integration. \square

References

- [1] Smets, B., Portegies, J., Bekkers, E. & Duits, R. PDE-based group equivariant convolutional neural networks. *Journal of Mathematical Imaging and Vision* **65**, 209–239 (2023). <https://doi.org/10.1007/s10851-022-01114-x>.

- [2] Cohen, T. & Welling, M. *Group equivariant convolutional networks*. (eds Balcan, M. F. & Weinberger, K. Q.) *Proceedings of The 33rd International Conference on Machine Learning*, Vol. 48 of *Proceedings of Machine Learning Research*, 2990–2999 (PMLR, New York, New York, USA, 2016). URL <https://proceedings.mlr.press/v48/cohen16.html>.
- [3] Staal, J., Abramoff, M., Niemeijer, M., Viergever, M. & van Ginneken, B. Ridge-based vessel segmentation in color images of the retina. *IEEE Transactions on Medical Imaging* **23**, 501–509 (2004). <https://doi.org/10.1109/TMI.2004.825627>.
- [4] Pai, G., Bellaard, G., Smets, B. & Duits, R. *Functional properties of PDE-based group equivariant convolutional neural networks*. (eds Nielsen, F. & Barbaresco, F.) *Geometric Science of Information*, 63–72 (Springer Nature Switzerland, Cham, 2023). https://doi.org/10.1007/978-3-031-38271-0_7.
- [5] Bellaard, G., Bon, D., Pai, G., Smets, B. & Duits, R. Analysis of (sub-)Riemannian PDE-G-CNNs. *Journal of Mathematical Imaging and Vision* **65**, 819–843 (2023). <https://doi.org/10.1007/s10851-023-01147-w>.
- [6] Bellaard, G., Pai, G., Bescos, J. & Duits, R. *Geometric adaptations of PDE-G-CNNs*. (eds Calatroni, L., Donatelli, M., Morigi, S., Prato, M. & Santacesaria, M.) *Scale Space and Variational Methods in Computer Vision*, 538–550 (Springer International Publishing, Cham, 2023). https://doi.org/10.1007/978-3-031-31975-4_41.
- [7] Field, D., Hayes, A. & Hess, R. Contour integration by the human visual system: Evidence for a local “association field”. *Vision Research* **33**, 173–193 (1993). [https://doi.org/10.1016/0042-6989\(93\)90156-Q](https://doi.org/10.1016/0042-6989(93)90156-Q).
- [8] Petitot, J. The neurogeometry of pinwheels as a sub-Riemannian contact structure. *Journal of Physiology - Paris* **97**, 265–309 (2003). <https://doi.org/10.1016/j.jphysparis.2003.10.010>.
- [9] Citti, G. & Sarti, A. A cortical based model of perceptual completion in the roto-translation space. *Journal of Mathematical Imaging and Vision* **24**, 307–326 (2006). <https://doi.org/10.1007/s10851-005-3630-2>.
- [10] Haar Romeny, B. *Front-End Vision and Multi-Scale Image Analysis* (Springer Dordrecht, 2003). <https://doi.org/10.1007/978-1-4020-8840-7>.
- [11] Iijima, T. Basic theory of pattern observation. *Papers of Technical Group on Automata and Automatic Control* (1959).
- [12] Weickert, J., Ishikawa, S. & Imiya, A. Linear scale-space has first been proposed in japan. *Journal of Mathematical Imaging and Vision* **10**, 237–252 (1999). <https://doi.org/10.1023/A:1008344623873>.
- [13] Koenderink, J. The structure of images. *Biological Cybernetics* **50**, 363–370 (1984). <https://doi.org/10.1007/BF00336961>.
- [14] Brockett, R. & Maragos, P. *Evolution equations for continuous-scale morphology*. (ed. IEEE) *1992 IEEE International Conference on Acoustics, Speech, and Signal Processing*, Vol. 3, 125–128 vol.3 (IEEE, 1992). <https://doi.org/10.1109/ICASSP.1992.226260>.
- [15] Evans, L. *Partial Differential Equations* Graduate studies in mathematics (American Mathematical Society, 2010). <https://doi.org/10.1090/gsm/019>.
- [16] Mohamed, M., Cesa, G., Cohen, T. & Welling, M. A data and compute efficient design for limited-resources deep learning (2020). <https://doi.org/10.48550/arXiv.2004.09691>.
- [17] Cohen, T., Weiler, M., Kicanaoglu, B. & Welling, M. *Gauge equivariant convolutional networks and the icosahedral CNN*. (eds Chaudhuri, K. & Salakhutdinov, R.) *Proceedings of the 36th International Conference on Machine Learning*, Vol. 97, 1321–1330 (PMLR, 2019). URL <https://proceedings.mlr.press/v97/cohen19d.html>.

- [18] Sosnovik, I., Szmaja, M. & Smeulders, A. *Scale-equivariant steerable networks*. (ed. ICLR) *International Conference on Learning Representations* (ICLR, 2020). URL <https://openreview.net/forum?id=HJgpugrKPS>.
- [19] Lindeberg, T. Scale-covariant and scale-invariant gaussian derivative networks. *Journal of Mathematical Imaging and Vision* **64**, 223–242 (2022). <https://doi.org/10.1007/s10851-021-01057-9>.
- [20] Worrall, D. & Welling, M. *Deep scale-spaces: Equivariance over scale*. (eds Wallach, H. et al.) *Advances in Neural Information Processing Systems*, Vol. 32 (Curran Associates, Inc., 2019). URL https://proceedings.neurips.cc/paper_files/paper/2019/file/f04cd7399b2b0128970efb6d20b5c551-Paper.pdf.
- [21] Sangalli, M., Blusseau, S., Velasco-Forero, S. & Angulo, J. *Scale equivariant neural networks with morphological scale-spaces*. (eds Lindblad, J., Malmberg, F. & Sladoje, N.) *Discrete Geometry and Mathematical Morphology*, 483–495 (Springer International Publishing, Cham, 2021). https://doi.org/10.1007/978-3-030-76657-3_35.
- [22] Pauwels, E., van Gool, L., Fiddelaers, P. & Moons, T. An extended class of scale-invariant and recursive scale space filters. *IEEE Transactions on Pattern Analysis and Machine Intelligence* **17**, 691–701 (1995). <https://doi.org/10.1109/34.391411>.
- [23] Duits, R., Florack, L., Haar Romenij, B. & Graaf, H. *Scale-space axioms critically revisited*. (ed. Younan, N.) *Proceedings of the Fourth IASTED International Conference on Signal and Image Processing*, 304–309 (ACTA Press, Canada, 2002).
- [24] Welk, M. *Families of generalised morphological scale spaces*. (eds Griffin, L. & Lillholm, M.) *Scale Space Methods in Computer Vision*, 770–784 (Springer, Berlin, Heidelberg, 2003). https://doi.org/10.1007/3-540-44935-3_54.
- [25] Schmidt, M. & Weickert, J. Morphological counterparts of linear shift-invariant scale-spaces. *Journal of Mathematical Imaging and Vision* **56**, 352–366 (2016). <https://doi.org/10.1007/s10851-016-0646-8>.
- [26] Heijmans, H. & Boomgaard, R. Algebraic framework for linear and morphological scale-spaces. *Journal of Visual Communication and Image Representation* **13**, 269–301 (2002). <https://doi.org/10.1006/jvci.2001.0480>.
- [27] Fathi, A. & Maderna, E. Weak KAM theorem on non compact manifolds. *Nonlinear Differential Equations and Applications NoDEA* **14**, 1–27 (2007). <https://doi.org/10.1007/s00030-007-2047-6>.
- [28] Azagra, D., Ferrera, J. & López-Mesas, F. Nonsmooth analysis and Hamilton–Jacobi equations on Riemannian manifolds. *Journal of Functional Analysis* **220**, 304–361 (2005). <https://doi.org/10.1016/j.jfa.2004.10.008>.
- [29] Alvarez, L., Guichard, F., Lions, P. & Morel, J. Axioms and fundamental equations of image processing. *Archive for Rational Mechanics and Analysis* **123**, 199–257 (1993). <https://doi.org/10.1007/BF00375127>.
- [30] Sapiro, G. *Geometric Partial Differential Equations and Image Analysis* (Cambridge University Press, 2001). <https://doi.org/10.1017/CBO9780511626319>.
- [31] Citti, G., Franceschiello, B., Sanguinetti, G. & Sarti, A. Sub-riemannian mean curvature flow for image processing. *SIAM Journal on Imaging Sciences* **9**, 212–237 (2016). <https://doi.org/10.1137/15M1013572>.
- [32] Guichard, F. & Morel, J. *Partial differential equations and image iterative filtering*. (eds Duff, I. & Watson, G.) *The State of the Art in Numerical Analysis*, Vol. 63, 252–562 (Clarendon Press, 1997). <https://doi.org/10.1093/oso/9780198500148.003.0020>.
- [33] Dorst, L. & Boomgaard, R. Morphological signal processing and the slope transform.

- Signal Processing* **38**, 79–98 (1994). [https://doi.org/10.1016/0165-1684\(94\)90058-2](https://doi.org/10.1016/0165-1684(94)90058-2).
- [34] Florack, L. Non-linear scale-spaces isomorphic to the linear case with applications to scalar, vector and multispectral images. *International Journal of Computer Vision* **42**, 39–53 (2001). <https://doi.org/10.1023/A:1011185417206>.
- [35] Felsberg, M. & Sommer, G. The monogenic scale-space: A unifying approach to phase-based image processing in scale-space. *Journal of Mathematical Imaging and Vision* **21**, 5–26 (2004). <https://doi.org/10.1023/B:JMIV.0000026554.79537.35>.
- [36] Duits, R., Florack, L., de Graaf, J. & Haar Romenij, B. On the axioms of scale space theory. *Journal of Mathematical Imaging and Vision* **20**, 267–298 (2004). <https://doi.org/10.1023/B:JMIV.0000024043.96722.aa>.
- [37] Yosida, K. *Functional Analysis* (Springer Berlin, Heidelberg, 1965). <https://doi.org/10.1007/978-3-662-25762-3>.
- [38] Burgeth, B. & Weickert, J. An explanation for the logarithmic connection between linear and morphological system theory. *International Journal of Computer Vision* **64**, 157–169 (2005). <https://doi.org/10.1007/s11263-005-1841-z>.
- [39] Akian, M., Quadrat, J. & Viot, M. *Bellman processes*. (eds Cohen, G. & Quadrat, J.) *11th International Conference on Analysis and Optimization of Systems Discrete Event Systems*, 302–311 (Springer Berlin Heidelberg, Berlin, Heidelberg, 1994). <https://doi.org/10.1007/BFb0033561>.
- [40] Pin, J.-E. in *Tropical Semirings* (ed. Gunawardena, J.) *Idempotency (Bristol, 1994)* Publ. Newton Inst. 11, 50–69 (Cambridge Univ. Press, Cambridge, 1998). URL <https://hal.science/hal-00113779>.
- [41] saz. Measurability of a pointwise limit of measurable functions. Mathematics Stack Exchange. URL <https://math.stackexchange.com/q/921576>.
- [42] Matematleta. a proof that the pointwise limits of lower semicontinuous (lsc) functions is lsc. Mathematics Stack Exchange. URL <https://math.stackexchange.com/q/2968282>.
- [43] Kolokoltsov, V. & Maslov, V. *Idempotent Analysis and Its Applications* (Springer Dordrecht, 1997). <https://doi.org/10.1007/978-94-015-8901-7>.
- [44] Rudin, W. *Functional Analysis* (McGraw-Hill, 1973, 1991).
- [45] Kraakman, T. B. *On the Construction of Classical and Quantum PDE-Based Neural Networks*. Master’s thesis, Eindhoven University of Technology (2023).
- [46] Castella, A. *Introduction to Shift-Invariant PDE-based Convolutional Neural Networks and experimentation with Vessel Segmentation*. Bachelor’s thesis, Eindhoven University of Technology (2021).
- [47] Borwein, J. & Lewis, A. *Convex Analysis and Nonlinear Optimization* (Springer New York, NY, 2016). <https://doi.org/10.1007/978-0-387-31256-9>.